12-13-2008

Evaluation Of Chitosan And Collagen As Scaffolding For A Tissue Engineered Aortic Heart Valve

Steven Christopher Waller

EVALUATION OF CHITOSAN AND COLLAGEN AS SCAFFOLDING FOR A TISSUE ENGINEERED AORTIC HEART VALVE

By

Steven Christopher Waller

A Thesis
Submitted to the Faculty of
Mississippi State University
In Partial Fulfillment of the Requirements
for the Degree of Master of Science
in Biomedical Engineering
in the Department of Agricultural and Biological Engineering

Mississippi State, Mississippi

December 2008

EVALUATION OF CHITOSAN AND COLLAGEN AS SCAFFOLDING FOR A TISSUE ENGINEERED AORTIC HEART VALVE

By

Steven Christopher Waller

Approved:

Steven Elder Associate Professor of Agricultural and Biological Engineering Graduate Coordinator (Director of Thesis)	James N. Warnock Assistant Professor of Agricultural and Biological Engineering (Major Professor)
Robert Cooper Associate Dean of the College of Veterinarian Medicine (Committee Member)	Jun Liao Assistant Professor of Agricultural and Biological Engineering (Committee Member)
Sarah Rajala Dean of the College of Engineering	

Name: Steven Christopher Waller

Date of Degree: December 12, 2008

Institution: Mississippi State University

Major Field: Biomedical Engineering

Thesis Director: Dr. Steven Elder

Major Professor: Dr. James N. Warnock

Title of Study: EVALUATION OF CHITOSAN AND COLLAGEN AS SCAFFOLDING FOR A TISSUE ENGINEERED AORTIC HEART VALVE

Pages in Study: 67

Candidate for Master of Science

Children born with congenital heart valve defects require open-heart surgery to implant an artificial replacement valve. These valves are unable to grow with the developing child and need replacing every 5 years. Tissue engineered heart valves, capable of growing with the patient, would alleviate the need for repeat surgery. I hypothesize chitosan and collagen possess advantageous qualities as scaffolding for a tissue engineered heart valve. This study evaluated chitosan and collagen hydrogels as potential scaffold materials. Chitosan scaffolds had suitable pore size/distribution and scaffold strength; however, they were unable to sustain cell attachment or viability. Collagen gels were assessed for compaction, mechanical properties and expression of matrix metalloproteases in the presence or absence of biochemical and mechanical stimuli. Pressure increased the remodeling potential. This was augmented further in the

presence of TGF-β. In conclusion, both materials have potential as scaffolding substrate in a tissue engineered heart valve.

DEDICATION

I would like to dedicate this research to all that have invested in me. Your investments of money, effort and time have not gone unnoticed. Without your investments I would not be at this milestone, or the man I am today.

ACKNOWLEDGEMENTS

The author would like to offer his sincere thanks to the many people who have contributed to the success of this project. First, I would like to thank Dr. James Warnock for his input and guidance throughout this study. Also I would like thank the members of the thesis committee, Dr Steven Elder, Dr. Jun Liao, and Dr. Robert Cooper, for their time and input. To Scott Metzler, Katie Culpepper, Carol Pregenero, and Kimberly Schipke I would like to offer my heartfelt appreciation for their time, input and friendship. Finally, I would like to thank my parents Bill and Beverly Waller for their love and undying support of my endeavors throughout my life.

TABLE OF CONTENTS

LIST OF TABLES

TABLE

TABLE OF FIGURES

FIGURE

CHAPTER I

INTRODUCTION AND BACKGROUND

Physiology of the Heart

The heart is a four chamber organ that is responsible for pumping hormones, blood and nutrients throughout the body. Briefly, deoxygenated blood flows into the right atrium from the inferior and superior vena cava. The right atrium contracts pumping blood through the tricuspid valve into the right ventricle. The tricuspid valve closes to prevent backflow of blood into the right atrium. Upon filling of the right ventricle, blood is pumped through the pulmonary valve to the lungs via the pulmonary artery for oxygenation. The pulmonary vein returns oxygen rich blood to the left atrium. Next, the left atrium contracts pumping blood through the mitral valve to the left ventricle. Once the mitral valve closes, the left ventricle propels blood through the aortic valve and to the entire body. This process, and the anatomy of the heart, is shown in Figure 1. Before blood is expelled from the left ventricle, the aortic valve changes size and shape (1). This finding conflicts the previous notion that the aortic valve was passive and would open due to a pressure gradient. Once the ventricles relax, pressure in the left ventricle drops, causing blood to flow backwards. The result of this backflow causes the cusps to snap together, preventing regurgitation.

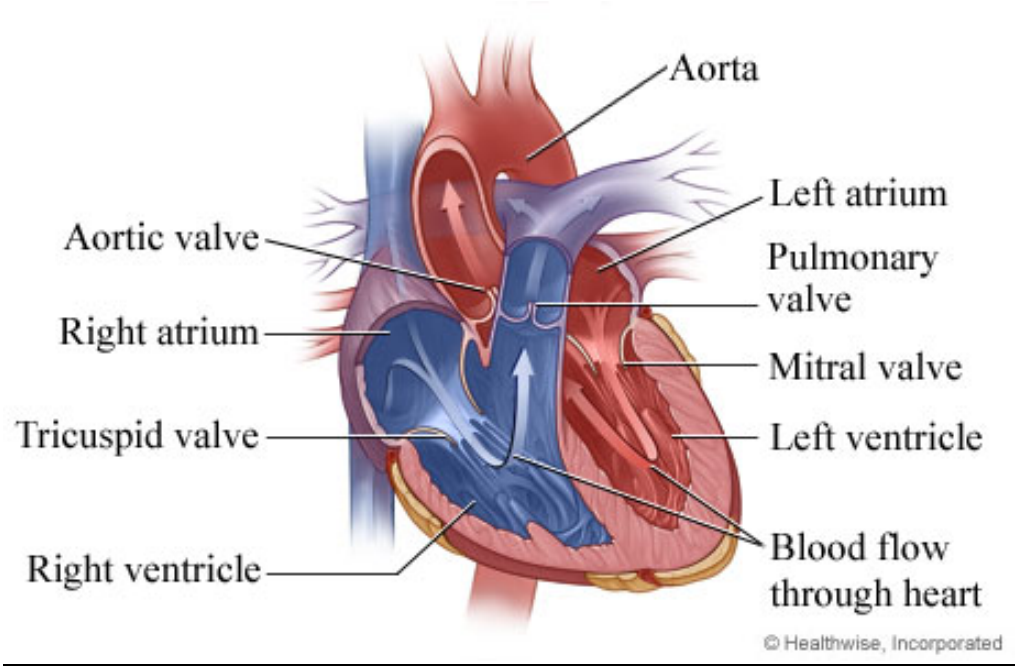

Figure 1 Blood flow through the heart with oxygenated blood in red and deoxygenated blood in blue (revolutionhealth.com)

Aortic Valve Structure

As the gateway of blood from the heart, the aortic valve is subject to many different forces and subsequently has a structure able to withstand these loads. The aortic valve consists of three leaflets and three sinuses. The leaflets resemble half moons thus, they are called semilunar. The sinuses are the areas behind the leaflets. At the lower end, the sinuses merge with the left ventricle, and the upper end is incorporated into the ascending aorta. The sinuses are named right coronary sinus, left coronary sinus, and noncoronary sinus. Figure 2 shows a representation of the aortic root opened longitudinally through the left coronary sinus. The junctions between the leaflets are known as commissures. The leaflet commissures are formed where two leaflets insert

side by side along parallel lines. The sinuses come together at the commissures and continue across the sinus rim distally into the aorta. As the ventricles contract during systole, the three semilunar cusps of the aortic valve are pushed aside, towards the walls of the aorta.

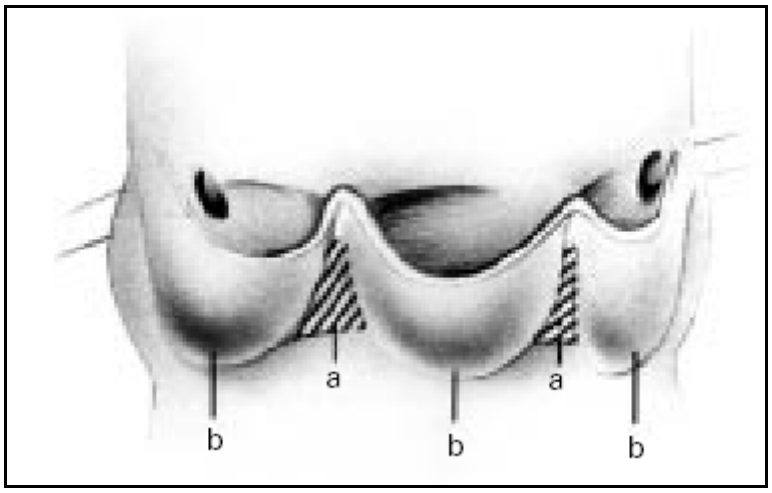

Figure 2 Aortic valve (a) intraleaflet triangles (b) leaflets

The aortic valve leaflets are flaps that seal the valve when it closes. Leaflets can be broken down into three regions, as shown in Figure 2. One region is known as the ventricularis, which is the layer that faces the left ventricle. The ventricularis comprises approximately 20% of the total thickness of the leaflet and consists of a dense network of collagen and elastin fibers. The middle gelatinous region of the leaflet is known as the spongiosa. Comprising 35% of the total valve thickness, the spongiosa contains a high concentration of glycosaminoglycans. The fibrosa, which constitutes 45% of the total thickness, faces the aorta and is subjected to sizeable amounts of shear stress due to the turbulent flow of blood coming from the left ventricle during systole. The fibrosa is

noticeably wavy as compared to the smooth ventricularis. For this reason, the fibrosa is composed predominately of a dense network of collagen fibers and thus able to withstand substantial amounts of stress as previously described (2). The fibrosa and ventricularis are also preloaded because of their attachment to each other. Due to this preloading, the fibrosa is under compression and the ventricularis is under tension (3).

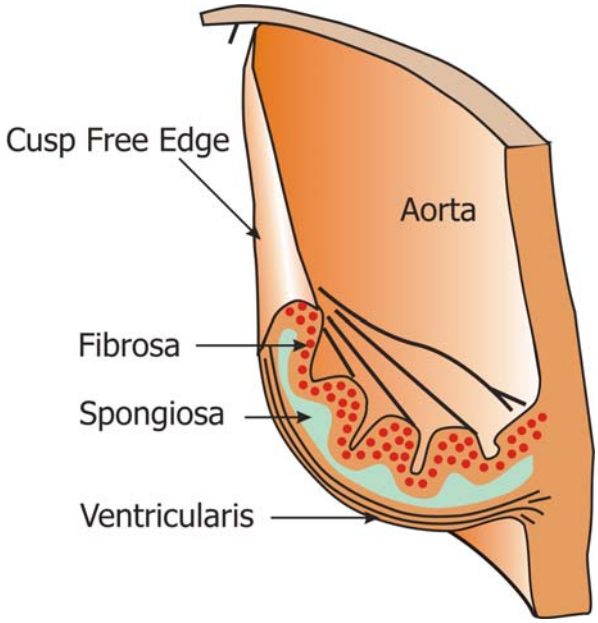

Figure 3 Layers of the aortic valve: the fibrosa faces the aorta and contains collagen fibers oriented in the circumferential direction; the spongiosa is the middle layer and is composed of mostly proteogylcans and glycosaminoglycans; the ventricularis faces the left ventricle and contains collagen and elastin fibers oriented in the radial direction (3).

Cells of the Aortic Valve Leaflet

The aortic valve consists of two distinct types of cells known as valvular interstitial cells (VICs) and endothelial cells (ECs). ECs line the surface of the leaflet and

create a nonthrombogenic blood-tissue interface. This interface allows ECs to regulate inflammatory and immune responses via biochemical signaling to interstitial cells. In addition, Filip *et al*. speculated that physical communication also occurs between ECs VICs. ECs are thought to regulate vascular tone, inflammation, thrombosis and remodeling. Disruption or damage to the EC monolayer is known to initiate an inflammatory response leading to valvular disorders.

Many differences exist between valve and vascular ECs. Valvular ECs align perpendicular to blood flow due the mechanical stress induced by the flow of blood, while vascular ECs align parallel to blood flow. Canine valvular ECs are oriented circumferentially across leaflets (4). In addition, aortic ECs have a distinct phenotype and gene expression profile compared to vascular ECs exposed to the same mechanical environment (5). Finally, different transcriptional profiles are exhibited by ECs harvested from the ventricularis and the fibrosa side (6).

VICs are more numerous than the previously described valvular ECs. VICs can be present in all the layers of the leaflet with various densities, and are responsible for organizing and remodeling matrix proteins. VICs possess a phenotypic plasticity that is regulated by environmental matrix stimuli and soluble signals (7). VICs can be further divided into myofibroblast, fibroblast and smooth muscle cells. The phenotypic state of valvular interstitial cells corresponds to the remodeling demand of the tissue, and has correlated cellular contractility to biosynthetic activity (8). Activated VICs, or myofibroblasts, are collagen producing cells that express contractile proteins, most notably α-smooth muscle actin. In normal healthy valves α-smooth muscle actin is present at low levels(9). However, valve remodeling causes VICs to express α-smooth

muscle actin at an elevated level (9;10). VICs assist in maintaining structural integrity of the leaflet tissue via remodeling by protein synthesis and enzymatic degradation. In addition fibroblasts synthesize collagen, proteoglycans, growth factors, elastin, cytokines, fibronectin, chemokines, and matrix metalloproteases (MMPs). Valvular MMPs control growth factor production and remodel extracellular matrix (ECM). Smooth muscle cells are found either singly or arranged in thin bundles and have been implicated in valvular contraction (11). Smooth muscle cells are characterized by the expression of α/β-myosin heavy chain and α-myosin heavy chain, SM1 and SM2 respectively. Myofibroblast are postulated to be involved in cellular contraction, migration and proliferation. Myofibroblasts show features of both smooth muscle cells and fibroblast by expressing contractile proteins, secreting ECM, and containing both muscle and non-muscle regulatory and structural proteins (9;12).

Aortic Valve Disease

The aortic valve regulates blood flow from the heart to the entire body thus, a compromise of the structure or function of this valve may have dire consequences. Generally, the non-rheumatic diseases of the aortic valve fall into two categories. First, aortic stenosis is known as the condition when blood flow is restricted from a constricted valve. This form of valve disease can be seen as a congenital abnormality or can be manifested later in the form of buildup of scar tissue and calcium. Symptoms of aortic valve stenosis include shortness of breath, angina, dizziness, and possible sudden death (13). A precursor to stenosis is aortic valve sclerosis (AVS). AVS is a condition of thickening and calcification of the normal aortic valve without obstruction to the left

ventricular outflow track. Evidence suggests that AVS is associated with an increased incidence of cardiovascular events, such as myocardial infarction, heart failure and stroke (14). The second type of aortic valve disease, aortic regurgitation, occurs when retrograde blood is allowed back into the ventricle during diastolic filling, reducing the net forward flow of blood. This form of valve disease is usually initiated from structural abnormalities. Often times the aorta stretches, thus the aortic leaflets are inadequate to prevent regurgitation. In addition to being seen individually, these two conditions can occur simultaneously. The improper functioning of the aortic valve requires the heart working harder to supply the body with the proper amount of oxygen and nutrients. Similar to an athlete increasing his strength or adding muscle through strenuous training and conditioning, so does the heart when it must overcome the shortcomings of a faulty aortic valve. As the heart works harder, the ventricular wall becomes thickened, eventually leading to left ventricle hypertrophy and ultimately congestive heart failure.

Congenital cardiovascular defects occur in approximately 1 percent of all live births and are the most common congenital malformations in newborns. Two of the more common defects are Marfan's Syndrome and Tetralogy of Fallot. Marfan's Syndrome is seen in about 1 in every 5000 births worldwide (15). The recognizable features of the syndrome include tall stature, joint hypermobility, mitral valve prolapse and skeletal abnormalities. Aortic dilatation leads to aortic regurgitation and ultimately to aortic dissection, which is the most serious complication. Another congenital heart defect, Tetralogy of Fallot, is when four heart defects occur at birth. These defects include a ventricular septal defect, pulmonary stenosis, right ventricular hypertrophy, and an

overriding aorta. Both previously mentioned congenital heart defects require surgical intervention.

Current Treatment Options

With the prevalence of aortic valve disease the necessity arises for a substitute for these defective or faulty valves. Due to late detection and intervention, the treatment for a diseased aortic valve is typically total replacement of the valve. More than 100,000 US patients every year need to have their dysfunctional or diseased valves replaced (16). Currently, a surgeon may choose to use a bioprosthetic or mechanical valve as a treatment option depending on the specific needs of the patient.

Bioprosthetic valves are a treatment option that entails an allograft or xenograft replacement. Allografts are valves taken from humans and are ideal replacements because these valves are structurally identical. When a non-viable allograft is taken from a donor upon autopsy, the valve is treated with antibiotics to sterilize and can be stored at 4ºC for weeks. The drawback to the nonviable valves is the inability to remodel and repair, which greatly reduces the lifetime of the replacement. A second allograft option is to obtain a viable valve from an organ donor and cryopreserved in dimethylsulfoxide to protect from crystallization. This form of allograft is preferred because less deterioration has occurs. In general, allografts are preferred over xenografts; however, the supply of allografts is limited by the amount of donors and difficulty in acquiring the proper size. Ultimately, the supply does not meet the demand thus the need for xenografts.

Xenografts, which can be seen in Figure 4, are taken from another species, treated and implanted into the human body. Most often porcine aortic valves are chosen for the

structural and hemodynamic similarities. In addition, porcine aortic valves are readily available leading to an ample supply of replacements. Another xenograft option is a bovine pericardial valve and is fabricated from 3 separate pieces of calf pericardium treated in glutaraldehyde. The pieces are attached to a supporting stent and sewing cuff. In order to implant the valve into a human, the porcine or bovine valve is crosslinked with low concentrations of glutaraldehyde to reduce antigenicity and proteolytic degradation that would otherwise occur following implantation into the patient. Consequently, the treatment in glutaraldehyde kills the cells within the valve, and can lead to calcification and stiffening causing the need for still another option of replacement. Since the prosthesis no longer contains living cells, the valve cannot remodel or respond to injury as does normal, viable tissue.

Figure 4 Xenograft Options for Aortic Valve Replacement. A-B(medtronic) C(edwards.com) Stented Porcine Xenograft (A), Non-stented Porcine Xenograft (B), Bovine Pericardial Xenograft (C)

Another alternative for a diseased or malformed aortic valve is to undergo the Ross Procedure. The Ross Procedure entails using the pulmonary valve of the patient, an autograft, to replace the defected aortic valve. The pulmonary valve would then be replaced with a cryoperserved pulmonary valve from a cadaver. An advantage of the

Ross Procedure includes eliminating the risk of an immunogenic response from the implant. The valve is viable allowing remodeling and response to injury. Anticoagulation therapy is not needed for this procedure allowing for an active lifestyle. The longevity of this alternative is greater than a porcine prosthesis because the procedure is glutaraldehyde-free.

Mechanical valves are the second replacement option. Mechanical valves are composed of nonphysiologic biomaterials that employ a rigid, mobile occluder in a metallic cage as in the Bjork-Shiley, Hall-Medtronic, and OmniScience valves. A second type of tilting disk valve uses two carbon disks that are attached to a carbon ring as in the St. Jude Medical, CarboMedics CPHV, Medical Carbon Research Institute or On-X prosthesis. These types of aortic valve replacements can be seen in Figure 5. Pyrolytic carbon has excellent biocompatibility with thromboresistence, high fatigue strength, and wear resistance. The valves open and close passively due to the changes in pressure and blood flow within the chambers of the heart. The primary drawback of mechanical valve replacement is the patients need for lifelong anticoagulation therapy to reduce the risk of thrombosis and thromboembolic events that result from platelet activation due to turbulent flow through the valve (17). The turbulent flow through these mechanical valves creates large amounts of shear on vessel walls, which damages the endothelium. Platelets become activated and adhere when damage to the endothelium is encountered. A thrombus soon forms restricting blood flow through the vessel. Also, a major limitation in pediatric patients is the valve's inability to grow with the patient, which necessitates multiple surgeries throughout the patient's lifespan with an increase risk in

mortality with each subsequent surgery. An evaluation of current aortic valve replacements is seen in Table 1.

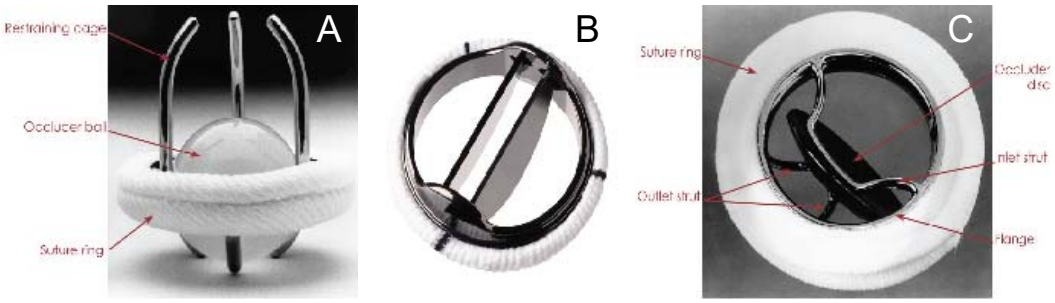

Figure 5 Mechanical Valves. Ball and Cage (A), Bileaflet tilting disc (B), Tilting Disc (C)

Table 1 Evaluation of current aortic valve replacements.

Mechanical Valves	Xenograft	Allograft	Ross Procedure
Foreign body response Lack of growth Mechanical failure Need for life long anticoagulation Thrombosis	Foreign body response Lack of growth Short durability Calcification	Foreign body response Lack of growth Donor organ scarcity Rejection	Foreign body response Growth potential No rejection

Tissue Engineering

Tissue engineering is an emerging field of medical science that fuses basic engineering and biology to create new organ or tissue for implantation. This new field offers a possible solution that would solve the short comings of current valvular treatment

options. As defined by Simmons *et al*. broad definition of tissue engineering is a set of tools at the interface of the biomedical and engineering sciences that use living cells or attract endogenous cells to assist tissue formation or regeneration, and thereby create therapeutic or diagnostic benefit (18). In most cases, cells are seeded onto a porous, biocompatible, and biodegradable scaffold. These constructs are allowed to grow and develop *in vitro* in a bioreactor prior to implantation. The ultimate goal is for the scaffold to gradually degrade as it is replaced by newly produced ECM as the tissue grows. Figure 6 illustrates a flow chart of the tissue engineering paradigm.

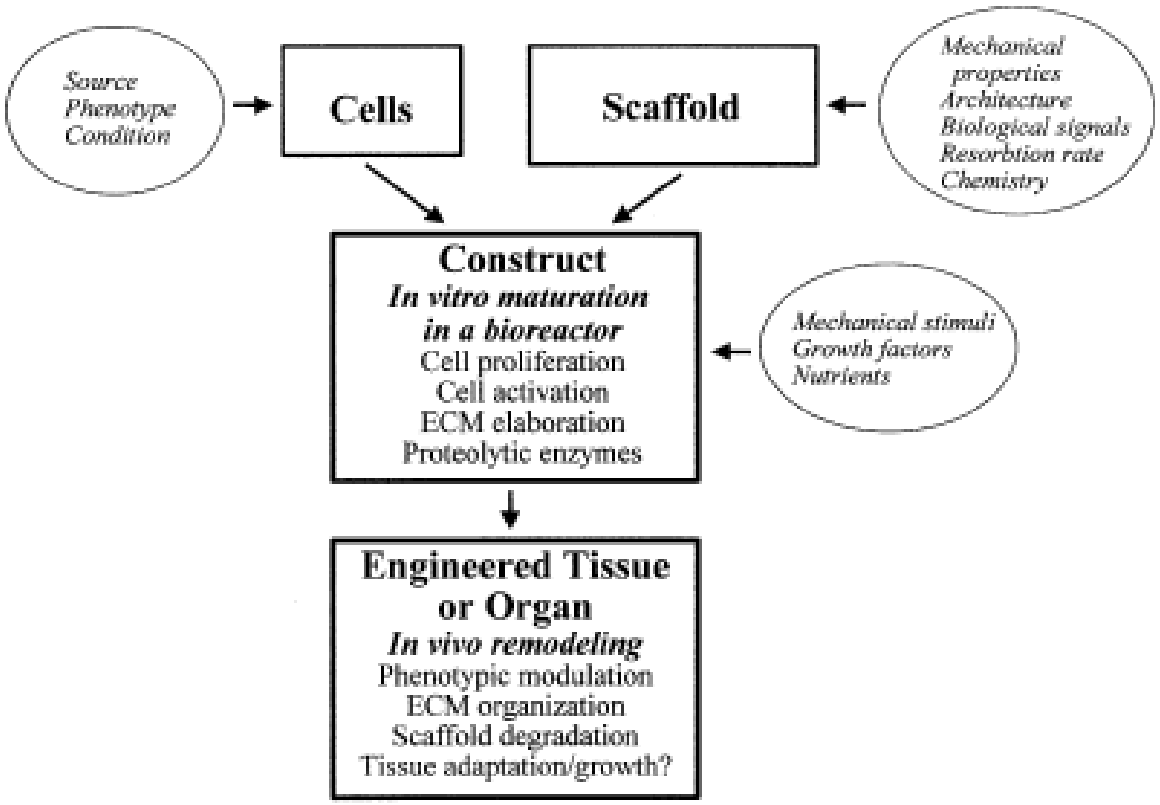

Figure 6 The tissue engineering paradigm is the logical progression from cell source to an implantable replacement. The paradigm begins with a decision into which cell source and material to use as scaffolding. The next progression is to mature the seeded construct *in vitro* before implantation. Finally, the engineered tissue is implanted in the patient and the construct undergoes *in vivo* remodeling to produce a functional replacement tissue or organ (19).

One of the first steps of engineering a tissue or organ is selecting a material to be used as a scaffold. The biomaterials used for this application have evolved through three generations. The first generation, beginning in the mid-20th century, of biomaterials were industrial materials that were not developed specifically for medical use. The goal of these materials was to be bioinert or elicit a minimal response from the host tissue. The

limited success of the first generation led to a development of a new generation of biomaterials. The second generation of biomaterials were intended to elicit a nontrivial and controlled reaction with the tissues in which they were placed to produce a desired therapeutic advantage. This generation also included resorbable biomaterials with variable rates of degradation to match the requirements of the intended application. The current or third generation of biomaterials are designed to stimulate precise reactions with proteins and cells at the molecular level. This generation establishes the scientific foundation for scaffolds to be seeded *in vitro* and subsequently implanted *in vivo* (19).

Scaffold Materials

Currently, many materials are being investigated to determine their potential use in tissue engineering. The ideal material is one that is biodegradable, bioresorbable, and elicits a minimal foreign body response. Investigators are looking into synthetic and biological derived polymers due to the ease of manufacturing and ability to control material properties.

Synthetic Polymers

Polyglycolic acid (PGA), an alpha polyester, has been used since the 1970s in reabsorbable sutures. Hutmacher *et al.* reported that PGA scaffolds degrade after approximately 8 weeks (20). However, PGA is broken down by hydrolysis, which causes a locally acidic environment. Due to the acidic conditions, degradation of PGA can produce a significant local inflammatory response(21). A second type of synthetic polymer is polylactic acid (PLA) which differs from PGA by one methyl group. PLA

exhibits more hydrophobic properties with less water uptake followed by a slower rate of hydrolysis due to the additional methyl group. PLA is used in sutures, staples and orthopedic devices. Compared to PGA, the inflammatory response to PLA is slightly less severe and has a longer resorption time of approximately 52 weeks (22).

Biological Polymers

Polyhydroxyalkanoates (PHAs) are naturally produced polyesters that are biosynthesized by various microorganisms. PHAs are a thermoplastic material that range from stiff and strong to flexible and ductile depending on composition. Degradation time of PHAs is approximately 52 weeks, as reported by Williams *et al,* and varies depending on composition, molecular weight and configuration(23). Poly-4-hydroxybutyrate (P4HB) is much stiffer than PHA and is processed using standard polymer processing techniques and has similar degradation times to PHAs.

Hypothesis and Objective

I hypothesize that chitosan and collagen have advantageous properties that make them ideal for scaffolding materials in a tissue engineered heart valve. With the drawbacks of current aortic valve replacements, a need for an alternative that can overcome these limitations has arisen. A possible solution to the shortcoming of current treatment options is the production of a tissue engineered aortic heart valve. One of the initial steps to engineering a tissue is determining the material that is biocompatible and biodegradable. The purpose of this study is to investigate the potential of chitosan and collagen hydrogels as scaffolding material for a tissue engineered heart valve.

CHAPTER II

METHODS AND MATERIALS FOR CELL CULTURE

Cell Isolation

Aortic valves were excised from freshly sacrificed pigs from a local abattoir (Sansing Meat Service, Maben, MS). The ventricles were removed by cutting laterally across the heart approximately half way up from the apex of the heart. The mitral valve was revealed and a cut was then made through the opening of the valve. The lower portion of the aortic valve was uncovered by the previous step. Once the valve was exposed, the valve was cut between commisures of the leaflets to reveal the three leaflets of the aortic valve. The leaflets were then removed by cutting around the cusp about one third up the leaflet to ensure no vascular tissue would be obtained. The hearts were rinsed in sterile phosphate buffered saline (PBS) (Sigma, St. Louis, MO) to eliminate blood and blood clots. The excised leaflets were transported to the laboratory in ice-cold PBS. Upon arrival at the laboratory, the leaflets were placed into a six well plate with one leaflet per well. Leaflets were then maneuvered to lay flat on the bottom of the well. Collagenase was made by creating a 1mg/mL solution of collagenase (Worthington, Lakewood, NJ) and Dulbecco's Modified Eagle Medium (DMEM) (Sigma, St. Louis, MO). Approximately 1 mL of collagenase solution was pipetted onto the flattened leaflets and placed in the incubator with 5% CO_2 and 37ºC. After 10 minutes of

incubation the ECs were removed by swabbing the leaflets with sterile swabs. These swabs were discarded or used for EC isolation. Next, the leaflets were placed into 10mL of collagenase solution and agitated overnight attached to a rotary bioreactor to gently agitate the leaflets. After 12-18 hours, the collagenase/leaflet suspension was centrifuged for 5 minutes at 1000 rpm and the supernatant was aspirated. The pellet of porcine VICs was then resuspended in complete media (DMEM, Sigma, St. Louis, MO, 10% FBS, Hyclone, Logan, UT, 1%Antibiotic-Antimyocyte, Sigma, St. Louis, MO) and the previous step was repeated. The resulting pellet was then resuspended in complete media (DMEM, 10%FBS, 1%ABAM) and plated onto a T-175 flask with 30 mL of complete media. Cells were grown to confluence as seen in Figure 7, then used or passaged out. Cells were maintained with standard cell culture techniques.

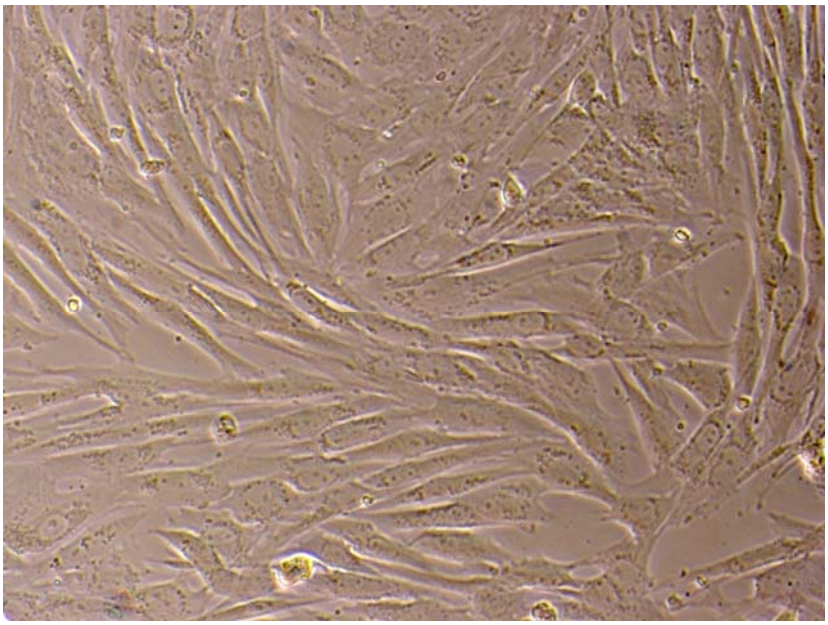

Figure 7 VICs grown to confluency in complete media on a T175 flask.

Cell Freezing

VICs were frozen to obtain a storehouse of viable cells. Freezing the cells required trypsinization of the growing cells from T-175 flask. To begin, the supernatant was aspirated off the cells contained within the near confluent T-175 flask. Next, a wash of approximately 10mL of PBS was performed to ensure that all complete media has been removed. Failure to rid the flask of media would cause trypsinization to be ineffective and inefficient. After rinsing, the PBS was aspirated off and 7 mL of trypsin (Sigma, St. Louis, MO) was pipetted into each flask. The flask with trypsin was then placed in an incubator for 7-10 minutes to allow for the detachment of cells from flasks. Extended exposure to trypsin has detrimental effects on cells. After the incubation time, 7 mL of complete media was added to each flask to inactivate the trypsin. The resulting solution was centrifuged for 10 minutes at 1000 rpm. The supernatant was removed and the resulting cell pellet was resuspended in complete media. A second centrifugation was performed and supernatant removed. The resulting pellet was resuspended in complete media so that the desired amounts of cells were in 1 mL of media per cryovial. Once in cryovials, 10% dimethyl sulfoxide (DMSO) (Sigma, St. Louis, MO) was added to each. The vials were immediately placed into a container partially filled with isopropenol to control the rate of freezing in the -80ºC freezer. After 24h the vials were removed from the isopropenol container and stored in a dry container within the -80ºC freezer.

Cell Thawing

Thawing cells required the removal of a cryovial from the -80ºC freezer. The vial was warmed by the heat emitted by the researcher's hand. Immediately upon thawing the

solution was placed into 10 mL of warm complete media. This was done to dilute the DMSO until it could be removed due to its detrimental effects on unfrozen cells. The dilute solution was centrifuged for 10 minutes at 1000 rpm. The supernatant was removed and the cell pellet was resuspended in the appropriate amount of complete media. The suspension was then plated onto desired flask and cultured as normal. Media was changed after 24 hours to eliminate cells that did not survive the thawing process.

CHAPTER III

EVALUATION OF CHITOSAN AS A BIOMATERIAL FOR TISSUE ENGINEERING

Introduction

Chitosan is an abundant biopolymer that is derived from shellfish, such as crab and shrimp. This biopolymer is considered industrial waste by the seafood industry which allows for an ample supply. Chitosan is formed when the number of N-glucosamine units is higher than 50%. When the amount of N-acetyl-glucosamine units is higher than 50% the molecule is known as chitin. Figure 8 depicts the molecular structure of chitin and chitosan. Chitosan, a linear polysaccharide, has been researched more than chitin due to its ability to be readily solubilized in dilute acid solutions. Source and preparation method dictate the molecular weight, which typically ranges from 300kD to 1000kD. In addition, commercially available chitosan has a degree of deacetylation of 50 to 90%.

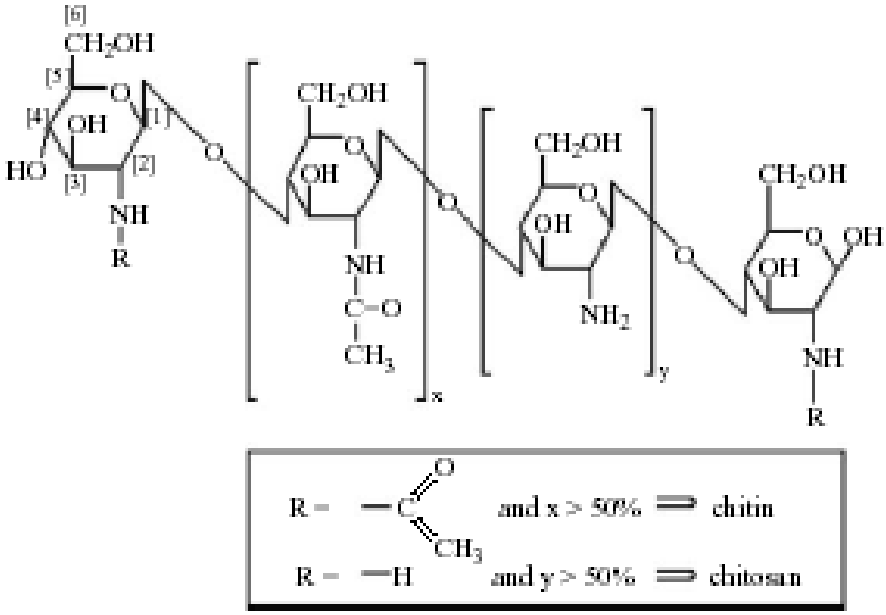

Figure 8 Molecular structure of chitin, a biopolymer from the exoskeletons of crustaceans, and chitosan, a readily solubilized, biocompatible biopolymer.

Chitosan shows great promise as a material for biomedical applications, including drug delivery, wound healing, and tissue engineering. The interest in chitosan is due to its excellent biocompatibility, biodegradation, and anti-inflammatory properties. Tomihata and Ikada studied the biocompatibility of chitosan *in vitro* and *in vivo* in rats (24). Their study demonstrated how the rate of degradation affected the biocompatibility of chitosan scaffolds. The study also revealed that as the degree of deacetylation increases, the rate of degradation decreases. This slower degradation rate did not elicit an inflammatory response as severe as the lower deacetylated (faster degrading) samples. The faster degradation causes an accumulation of degradation particles at the implant site, thus causing a more severe inflammatory response.

Chitosan is broken down into amino-sugars, which are excreted or incorporated into GAG or glycoprotein metabolic pathways (25). The body degrades chitin and its derivatives through enzymatic hydrolysis mediated by chitinase and lysozymes contained within macrophages (26). In addition, hydrolases can also breakdown chitin depending on the degree of deacetylation.

As of October 2008, a simple PubMed search of chitosan receives 5,234 hits, which demonstrates the interest in this biopolymer. While most research revolves around using chitosan in a drug delivery form, chitosan shows promise in many areas of tissue engineering. Jiankang *et al.* evaluated chitosan-gelatin hybrid scaffolds in hepatic tissue engineering (27). Nettles *et al.* explored chitosan as a potential material used for tissue engineering cartilage (28). Oliveira *et al.* studied the engineering of endochondral bone utilizing chitosan based scaffolds (29). Whereas, Blan *et al.* examined the possibility of using chitosan as a biomaterial to support the formation of contractile 3D heart muscle (30). Chitosan has also received some attention as a potential heart valve scaffold material (31).

Hypothesis and Objective

I hypothesize chitosan will possess strength similar to native decelluarized leaflets and cells will attach throughout the scaffold. The objective of this study is to evaluate chitosan as a material for a tissue engineered heart valve. The physical properties of chitosan scaffolds will be investigated to gain insight into the structure and performance of these scaffolds. Additionally, scaffolds will be produced and studied to determine if

scaffolds made from chitosan can support the attachment and growth of porcine aortic valve interstitial cells.

Methods and Materials

Chitosan (low molecular weight) (Sigma, St. Louis, MO) was dissolved (1%w/v) in Glacial Acetic Acid (Sigma, St. Louis, MO). The solution was stirred for 4-6 hours to ensure that chitosan was fully dissolved. The chitosan was then poured 1 mL per well into a 24 well plate. Next, the plate was placed into a -80ºC freezer for at least 24 hours. The samples were frozen at -80ºC rather than -20ºC, due to the effects of freezing rate on pore size and distribution (32). The freezing rate regulates the crystallization of water within the solution, thus, the size of the crystals dictate the pore size made upon lyophilization (32). Once frozen, the samples were lyophilized on a Flexi Dry (FTS Systems Inc., Stone Ridge, NY) for 24 hours. The scaffolds were rehydrated in a graded series of ethanol from 100 to 70%. At each step, the scaffolds were covered with enough of the appropriate ethanol to cover the samples and allowed to sit for approximately 30 minutes. Samples were cut into 5 X 10mm strips and remained in 70% ethanol for 2-6 hours to sterilize. Following sterilization, samples were rinsed twice in PBS.

Scaffold Preparation

Scaffolds were sterilized in 70% ethanol and then rinsed twice with sterile PBS to remove any residual ethanol. After rinsing with PBS, a 30 minute rinse in sodium hydroxide (0.1M NaOH) was conducted. This was performed to stabilize the scaffolds and create favorable environment for cells to attach. After removing the scaffolds from

NaOH, 3 mL of complete media was added to each scaffold and placed into an incubator 30 minutes prior to seeding.

Seeding Method

Three different methods for seeding were tried. The first method was blotting the scaffold dry before pipetting the cell suspension onto the scaffold. The scaffolds were allowed to sit undisturbed for 1 hour then 3 mL of complete media was added to each scaffold. A second method for seeding employed was an agitation method. This involved pipetting the cell suspension onto the scaffold and placing on a Belly Dancer Shaker (Stovall Life Sciences, Greensboro, NC) within an incubator. The third method of seeding was injecting cells into the scaffolds via a 20 gauge syringe and then placing into an incubator. One hour later 3 mL of complete media was added to each scaffold. The number of cells seeded onto scaffolds was 1, 3, or 5 million.

Scanning Electron Microscopy

Pore size was visualized and measured using scanning electron microscopy (SEM). Samples for SEM were fixed in 12.5%glutaraldehyde in 0.1M sodium cacodylate buffer. The samples were then rinsed in phosphate buffer, and post fixed with 2% Osmium tetraoxide in 0.1M phosphate buffer. Next, samples were dehydrated in a graded series of ethanol beginning at 50% ethanol and increasing by 25% each series. Each series lasted approximately 30 minutes. Samples were chemically dried using hexamethyldisilazane (HMDS) before air drying overnight. The dried samples were mounted on aluminum stubs, coated with gold/palladium, and viewed on a JEOL JSM-

6500F scanning electron microscope at 5kV. Images were taken at 300X and were exported with scale bars. Images were then analyzed in ImageJ (NIH) imaging software to determine an average pore size and distribution of pores. Pore size was measured by setting the scale with in ImageJ then overlaying lines on top of pores in the SEM image. In order to determine the average pore size a 20,000 μm^2 area was sectioned of by overlaying a rectangle on top of the image. Then pores within the quadrant were measured and averaged to give the average pore size.

Hematoxylin and Eosin Staining

To determine cell distribution and content, samples were stained with Hematoxylin and Eosin (H&E). Samples were first fixed in 10% buffered formalin for 1 hour then placed in PBS until staining. Samples were imbedded in paraffin and sectioned at a thickness of 10μm. The sections were then mounted to glass slides and prepared for staining. Staining began with submersion of slides in Clear-Rite 3 followed by submersion in a series of alcohol dilutions at 100, 95, and 70%, respectfully. Slides were rinsed by submersion in distilled water. Hematoxylin staining was then performed via submersion followed by a rinse in distilled water. Hematoxylin stained the nucleus blue. Next, the slides were submerged in 3% Glacial Acetic Acid and rinsed once again in distilled water. Submersion in a Bluing Solution was performed followed by a rinse in distilled water. The slides were then rinsed in 70% alcohol and then stained with Eosin Y solution. Eosin stained chitosan and collagen bright red. A rinse in 95% alcohol and absolute alcohol was performed. Slides were then submerged in Clear-Rite 3 twice.

Finally, cover-slips were applied using 1-2 drops of mounting medium. Slides were viewed by a light transmission microscope at 10X and 20X.

Laser Scanning Confocal Microscopy

Laser scanning confocal microscopy (LSCM) was performed by staining the scaffolds with 5μM calcein-AM and 5μM ethidium homodimer, which reveal live or dead cells, respectively. The stains were left on the scaffolds for approximately 15 minutes then rinsed in PBS. The scaffolds were then viewed on a Zeiss LSM 510 confocal microscope. The scaffolds were stained 24 hours after seeding to determine cell viability and number.

Dissolution Test

Degradation by hydrolysis was measured over an 8 week period. The rate and mode of degradation depends on the material deacetylation and crystallinity. Chitosan scaffolds with greater than 80% deacetylation and/or high crystallinity exhibit little degradation. To estimate the stability of chitosan scaffolds, a dissolution test was performed. These tests were performed by placing 6 scaffolds into a 50 mL tube, one scaffold per tube. Then 50 mL of media was added to the tube with either complete media or media without FBS and incubated. Over 8 weeks, the media was changed weekly and 10 mL was used to measure the kinematic viscosity. Samples incubated in the absence of FBS provided data on the degradation by hydrolysis, while tests performed in the presence of FBS provided information on the degradation by hydrolysis and serum

proteins/enzymes. The viscosity was measured using a capillary viscometer placed into a water bath regulated to 37ºC with an increase in viscosity indicating material degradation.

The capillary viscometer was loaded with the appropriate form of media and allowed to equilibrate to the temperature of the previously mentioned water bath. While placing a finger over the vent, the media was drawn up through the capillary past both indicator lines. The vacuum was then removed with a finger still over the vent. The finger was then removed and the efflux time for the fluid to flow downward from the top indicator line to the bottom indicator line was recorded. This process was performed 3 times per scaffold. To obtain the kinematic viscosity the recorded time was placed into the following equation:

$$\text{Kinematic Viscosity} = (\text{Viscometer constant X Efflux time}) \qquad \text{(Eq. 1)}$$

The viscometer constant was a known value that is derived by running a known substance through the viscometer. This value is typically provided by the manufacture. The kinematic viscosity of each scaffold was then averaged and plotted each week over an eight week period.

Chitosan Scaffold Tensile Testing

The tensile strength of the scaffolds was also evaluated by using the MACH1 micromechanical testing system as seen in Figure 9. Before tests were run, the 1kg load

cell was calibrated. The samples were placed into grips, which consisted of two steel plates held together by two nuts as seen in Figure 10. The testing sequence began by zeroing load cell and position to create a reference point. Next, the protocol called for a simple displacement, which was ran until failure of the scaffolds occurred.

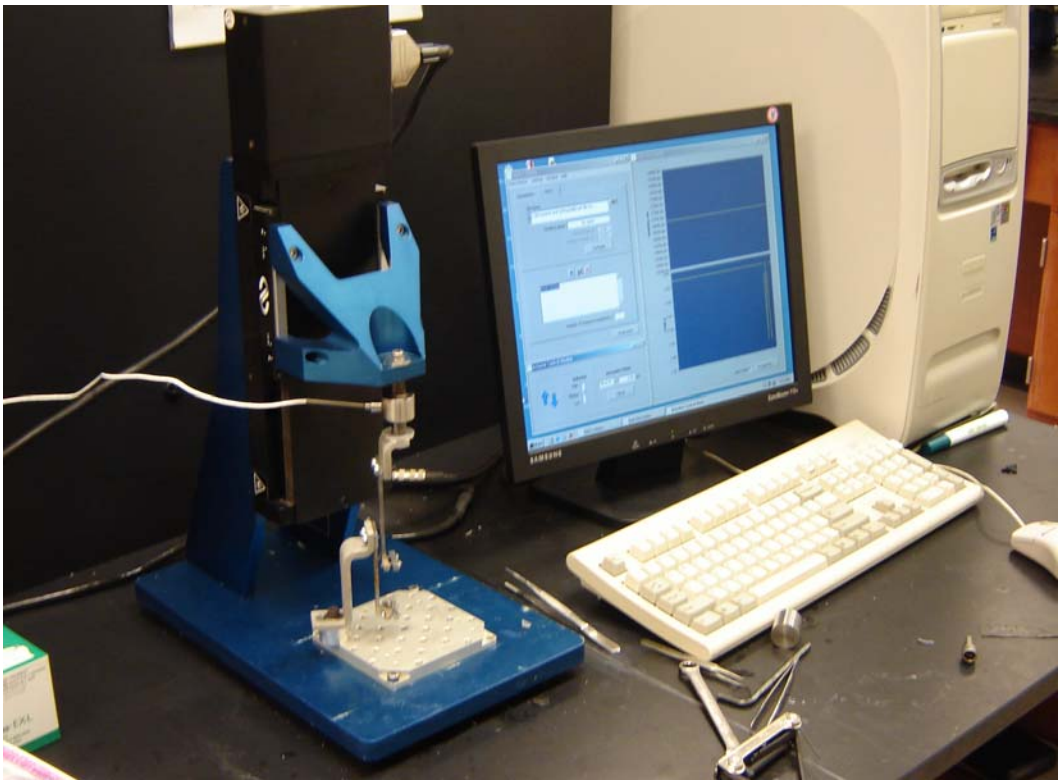

Figure 9 MACH1 micromechanical testing system used to evaluate the tensile strength of chitosan scaffolds.

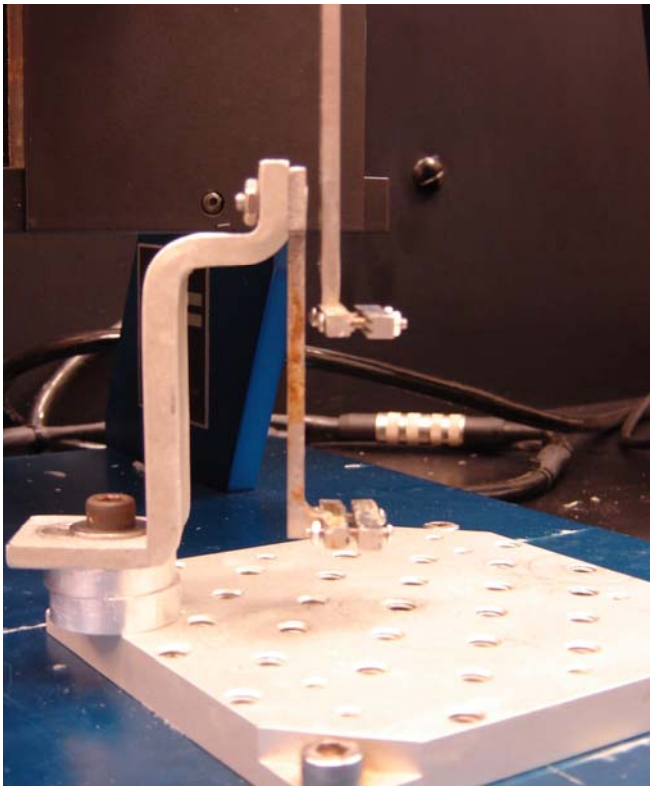

Figure 10: Clamps used to hold scaffolds while tensile test were perform. Two bolts drew the metal pieces together to clamp the scaffolds

Results

The chitosan scaffolds were analyzed under SEM to determine pore size. The scaffolds appeared to have uniform distribution of pores. Also, the scaffolds had sufficient pore size to accommodate VICs. The ideal pore size is deemed to be approximately 15 μm, which is a few microns larger than an average interstitial cell to allow for mass transport of nutrients and byproducts. SEM pictures confirm that pores were large enough for VICs to infiltrate and attach as seen in Figure 11, and pore diameter was measured. The average pore size was determined to be 18.76±7.75 μm. Further inspection of SEM pictures revealed fairly uniform distribution of pores.

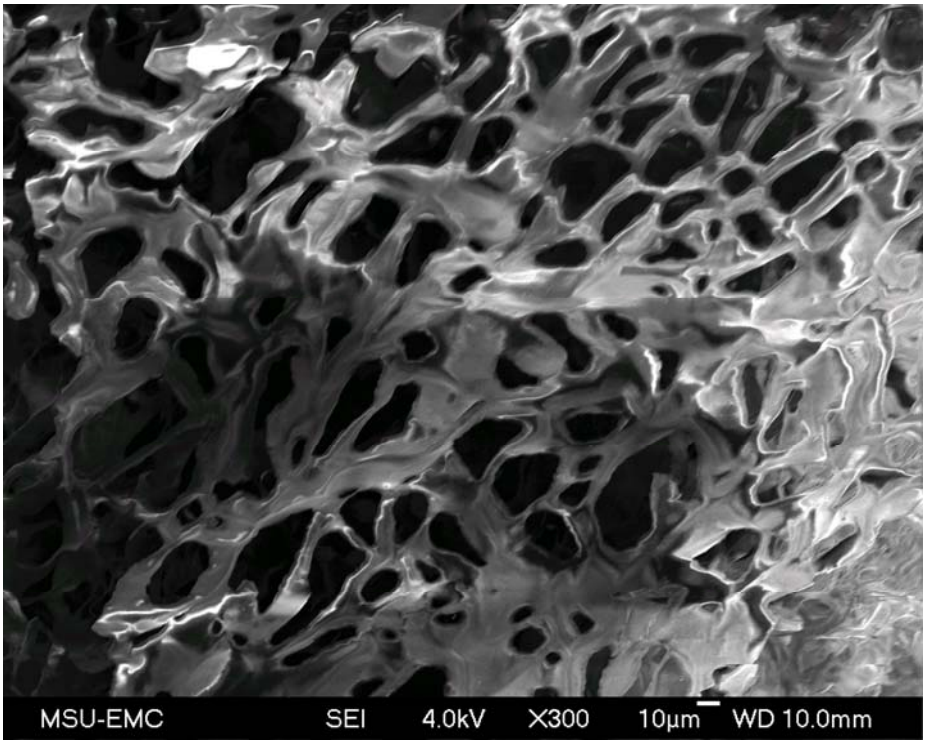

Figure 11 SEM image of chitosan scaffold, which reveals a favorable pore size and distribution.

H&E staining was conducted to determine the number of cells retained or attached to the scaffold and distribution of cells throughout the scaffold. H&E stained constructs can be seen in Figure 12 and13. H&E staining revealed ample pore space throughout the scaffolds. More cells were seen in scaffolds with a higher seeding density at various depths throughout the samples. However, the staining revealed extremely low cell counts overall, even from higher seeding densities.

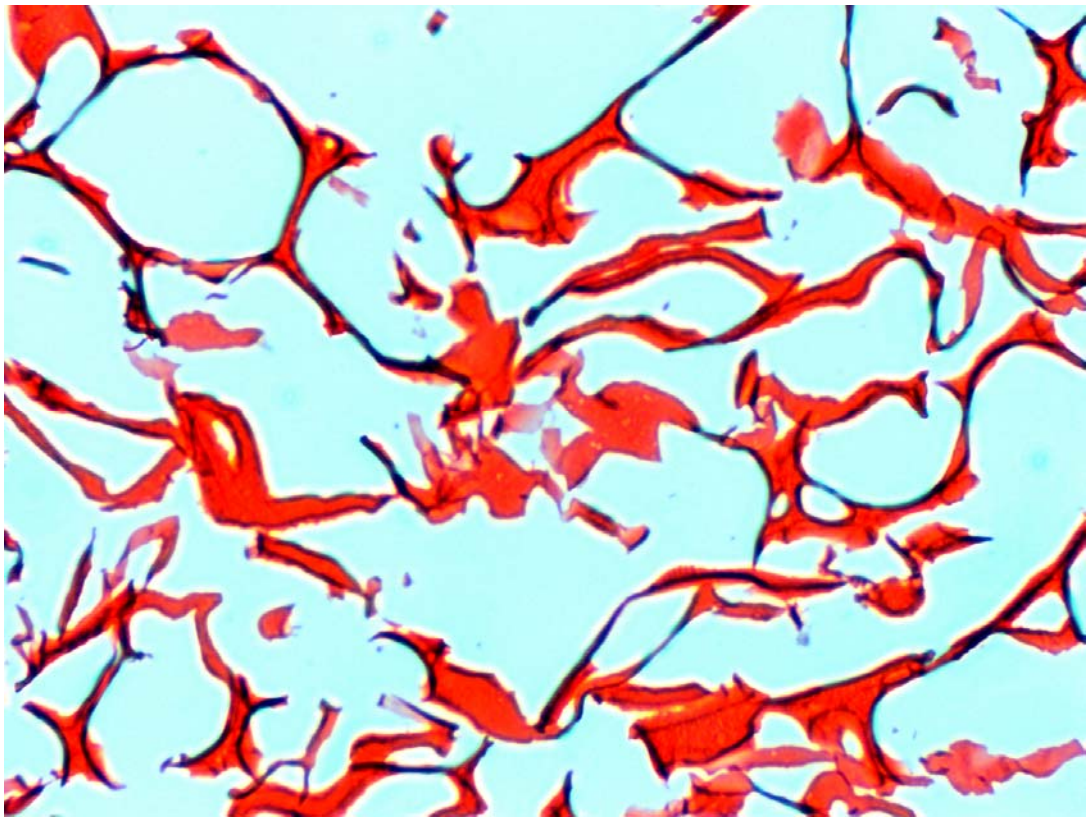

Figure 12 A section of a chitosan scaffold stained with H&E. The chitosan is stained red, and reveals ample pore distribution.

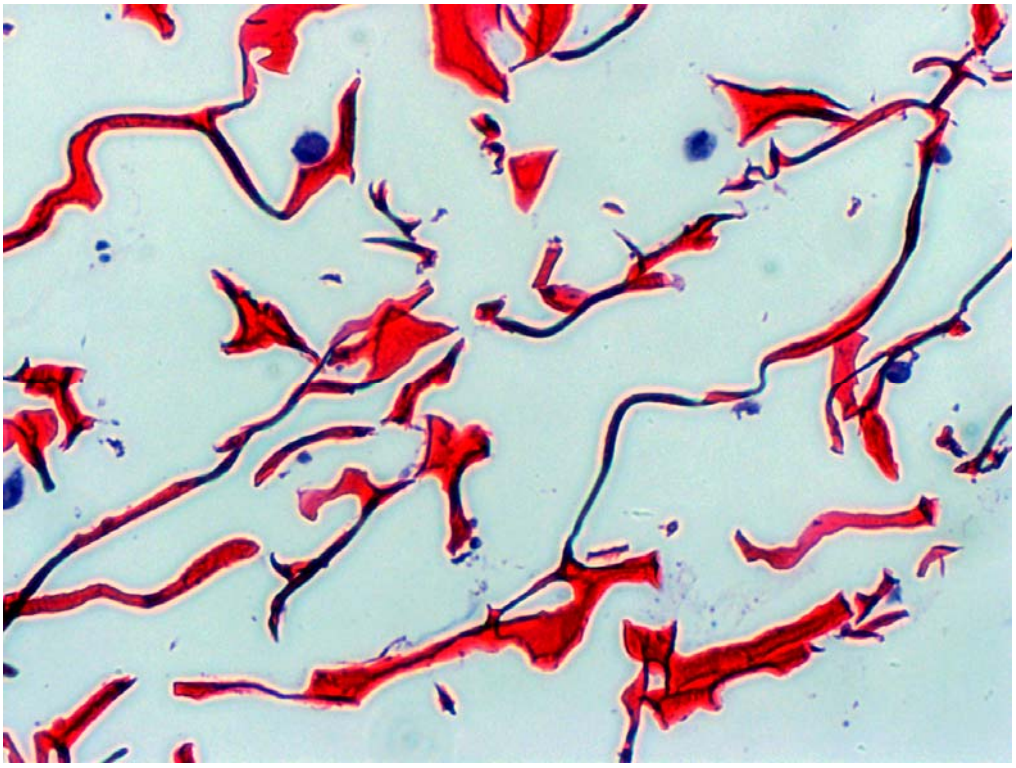

Figure 13 Section of chitosan stained with H&E after 72 hours. Chitosan is stained red and cells blue, and displays the cell distribution and infiltration into the scaffold. The scaffold was seeded via the agitation method with 3 million cells.

Confocal microscopy was performed on samples to determine cell number and viability. The Live/Dead staining of the scaffolds revealed that most of the cells seeded were dead within 24 hours. However, images obtained did show high cell retention or cell numbers. An example image of the Live/Dead staining of chitosan scaffolds can be seen in Figure 14.

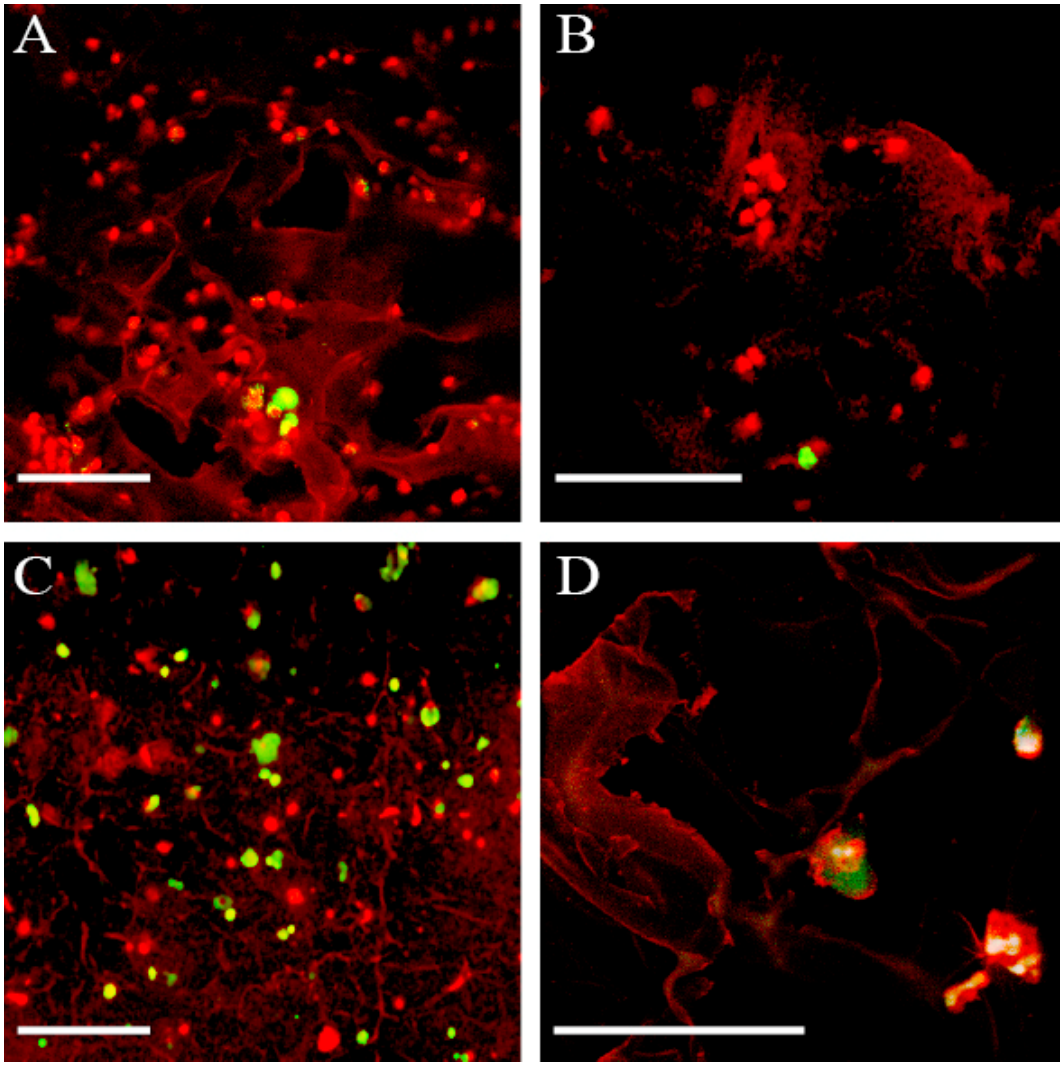

Figure 14 LSCM images of chitosan scaffolds prepared traditionally (A,B) and NaOH rinsed method(C,D). Live cells were stained with calcein-AM, which fluoresce green, while dead cells and autofluorescent chitosan are depicted in red. Images were taken 24 hours after seeding via injection. Scale bars represent 100 μm.

Chitosan autofluoresces red as seen above, and dead cells are stained red by eithidium homodimer. The numerous red dots or dead cells show good values of cells were seeded into the region. Also the new method of rinsing scaffolds in NaOH did result in a small amount of live cells, but the method still needs to be optimized to efficiently seed the scaffolds.

An average ultimate tensile strength of 0.0455±0.006 MPa over 6 samples was revealed from tensile testing. In addition, testing found an average elastic modulus of 0.1081±0.016 MPa. Table 2 shows the strength breakdown of the 6 matrices and Figure 15 is the stress versus strain curves.

Table 2 Table of strengths of 6 chitosan scaffolds measured via the MACH1

Scaffold	UTS (MPa)	Elastic Modulus (MPa)
Scaffold A	0.041086651	0.0846
Scaffold B	0.056835734	0.122
Scaffold C	0.046987665	0.099
Scaffold D	0.044920079	0.113
Scaffold E	0.043272502	0.128
Scaffold F	0.040496483	0.102
Average	0.0455 ± 0.006	0.1081 ± 0.016

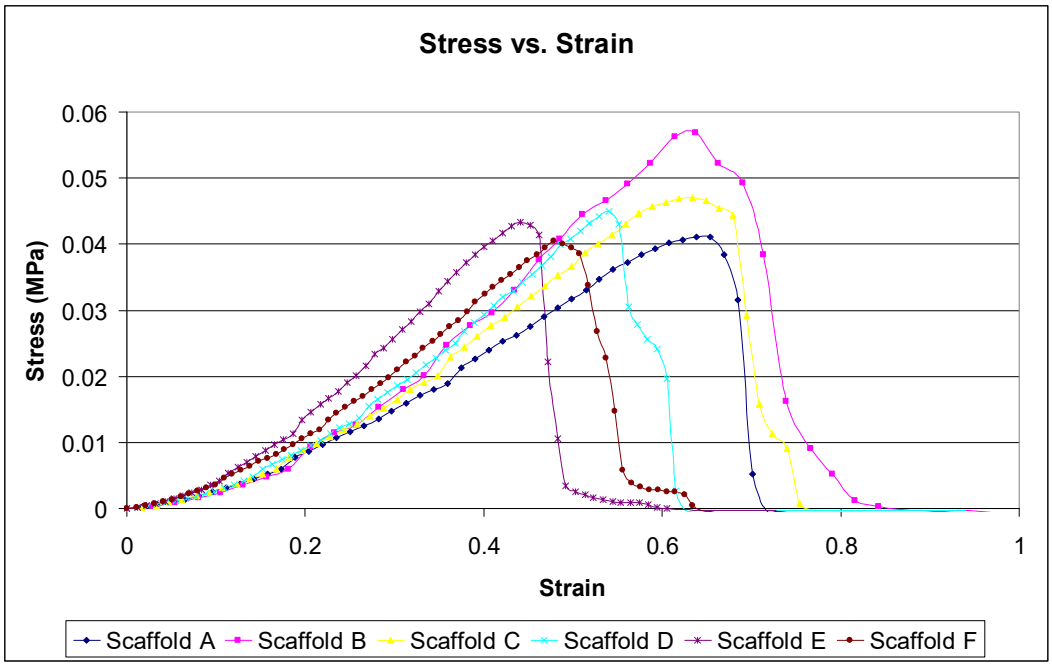

Figure 15 Stress vs. strain curves used to determine UTS and elastic moduli.

The eight week dissolution tests revealed that little to no degradation occurred. Visual inspection of scaffolds each week showed no evidence of degradation. The viscosity of the media with and without FBS showed no change throughout the eight week period. The lack of change of the viscosities of scaffolds in media without serum indicated that little degradation occurred through hydrolysis. In addition the minimal change of viscosities of scaffolds in media with FBS suggested no degradation of the scaffolds by serum proteins/enzymes. The viscosities over the eight weeks can be seen in Figures 16 and 17.

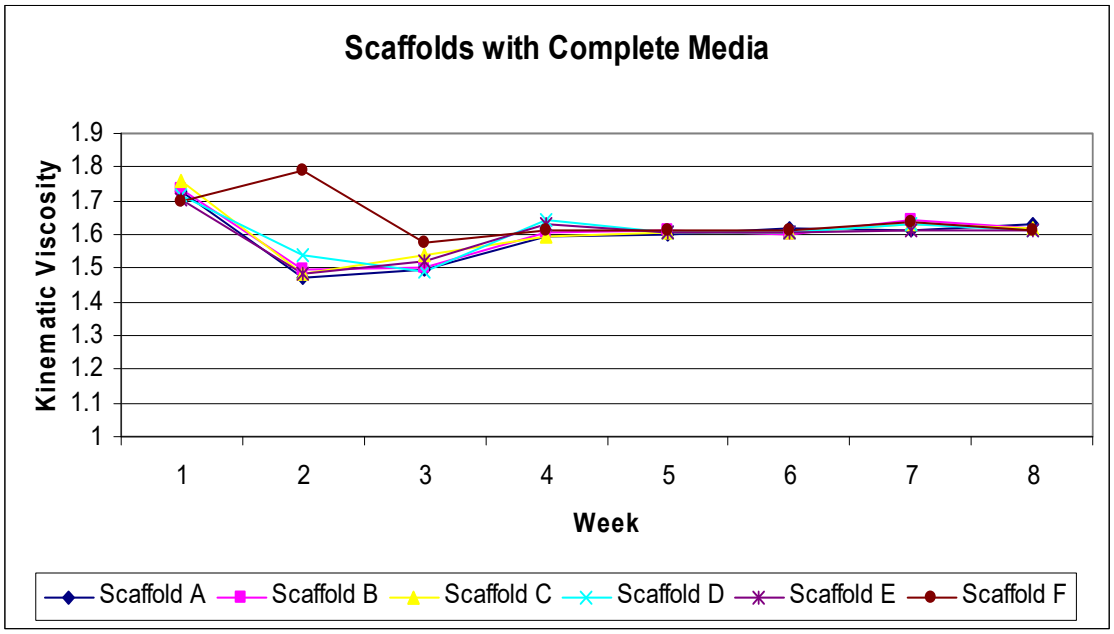

Figure 16 Change in viscosity of media with FBS over eight weeks

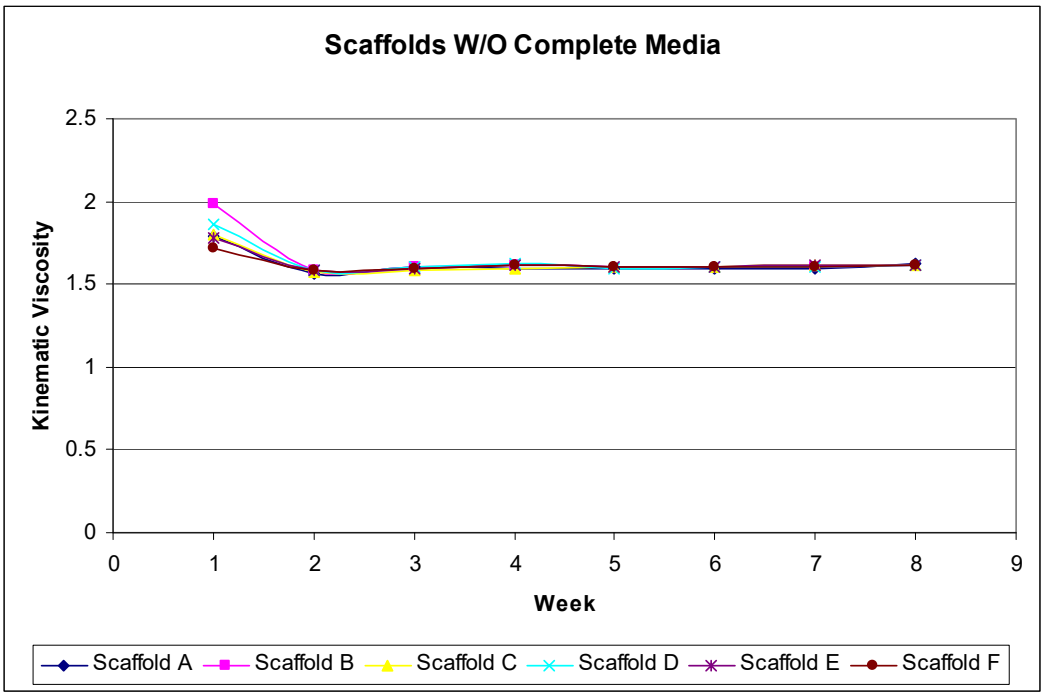

Figure 17 Change in viscosity of media without FBS over eight weeks

Discussion

While chitosan scaffolds are easily produced, there exists a large variation between scaffolds from batch to batch. Not only were variations seen from batch to batch, but also between wells as seen in the Figure 18, where image A shows pores with a different morphology/topography than image B. These variations possibly arrive due to impurities within the chitosan, or variations of external environmental conditions, such as relative humidity, temperature disparities, etc, when preparing the scaffolds.

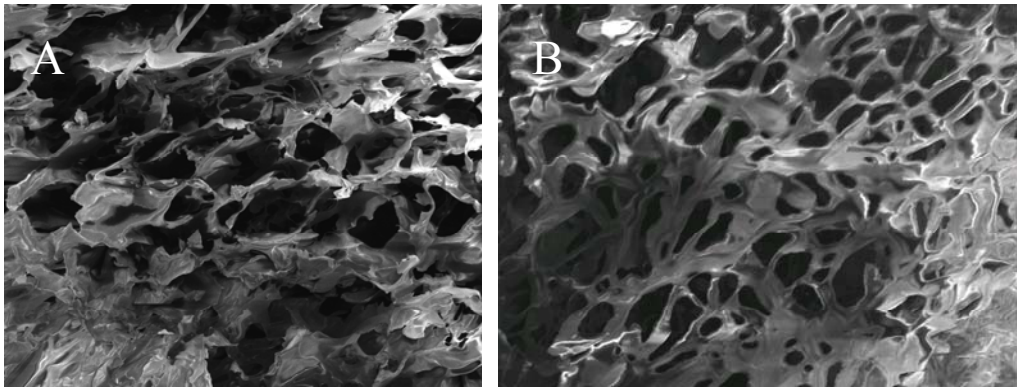

Figure 18 SEM images of chitosan scaffolds taken at 5kV on JOEL SEM , which show different morpholgoy/topography between samples. Image A shows a more random order of pores compared to the more uniformed pores in image B.

Difficulties arose when imaging due to the charge build up of the scaffolds, which causes the images to be distorted and less sharp. This could be overcome by a longer period of sputter-coating; however, lowering the voltage in which the image is taken can also allow for images to be taken at a lower quality. Also handling the scaffolds during preparation for SEM can damage the structure of the samples, which necessitates care when processing the samples. The pore size was found to be suitable for cell infiltration and mass transport. Also, pore distribution appeared uniform throughout the samples.

The method by which the scaffolds were created is widely accepted. The process of rehydration of scaffolds varies among researchers. Some researchers choose to change the ethanol concentration by 10% per series, while other use a 5% step. In addition, some groups choose to rinse the scaffolds in NaOH after rehydration. Each of these methods was explored with limited success. No difference could be discerned from the variation between size of steps in the previously mentioned ethanol series. However, when

chitosan was dissolved in 0.1M acetic acid live cells were seen attached on top of dead cells. The rinsing of scaffolds had the most promising results as seen in Figure 14.

LSCM was found to be a very useful tool in determining the overall outcome of seeding scaffolds. In addition, the autofluorescence of chitosan made viewing the pore size and distribution easy. Overall the number of cells attached was promising; however, lack of viable cells after 24 hours was a major concern. Once it was determined that the traditional method of scaffold preparation killed the seeded cells via a nonfavorable pH environment that was an artifact of the rehydration process, variations to the method were made. To eliminate the effects of ethanol on the scaffolds, the time spent at each interval in ethanol and number of PBS rinses before seeding was varied. This proved to only minimally improve the outcome of seeding. To aid in cell attachment, scaffolds were incubated in complete media prior to seeding, which gave serum proteins the opportunity to penetrate within the scaffold to aid in cell attachment. Each of these changes yielded a minimal amount of positive results. The only cells that were found viable were attached on top of another cell. This leads to the conclusion that the chitosan matrix was killing the cells. A new batch of chitosan solution was made from a higher grade chitosan. In addition, chitosan was dissolved in weaker acetic acid. None of these changes affected the fate of the cells. It was then suggested to rinse the scaffolds in 0.1M NaOH to stabilize the constructs and combat any residual pH issues from rehydration. This showed the most promising of the changes to the traditional method. As seen in Figure 14 cells seeded onto scaffolds that were rinsed in NaOH were viable after 12 hours. The results from a rinse in NaOH offer hope that further optimization of the seeding method and cell quantity can be made.

The mechanical data showed that scaffolds from the same batch had the same mechanical properties. The strength of chitosan scaffolds when compared to decelluarized and native valves is considerable lower (33). This means that the goal of creating a tissue that has the strength of native tissues is not met. Also the lack of strength suggests that a chitosan scaffold would not perform well under physiological loading.

The dissolution test revealed scaffolds do not degrade over a period of 8 weeks. Both scaffolds in media with or without FBS showed no signs of degradation. Since the viscosity of the media that was removed each week remained constant, it can be concluded that the majority of degradation is performed by enzymes within the body. Degradation of scaffolds by hydrolysis or serum protein/enzymes does not have an apparent effect on the overall degradation.

Current literature suggests chitosan appears to have a lot of potential as a biomaterial for tissue engineering constructs. The biocompatibility and favorable degradation of chitosan makes it an interesting material to research for biomedial applications. However, the variation between batches and detrimental effects on VICs causes one to reassess the use of chitosan for this application.

Conclusion

Chitosan, as expected, was easily processed and made into scaffolds. The study revealed good pore size and distribution throughout the scaffolds. Also, a cell distribution throughout the scaffolds was shown in H&E staining. However, cell viability was a major drawback of using traditional methods for processing chitosan scaffolds.

Live/Dead staining displayed large quantities of dead cells. A NaOH rinse of rehydrated scaffolds increased the number of viable cells; however, further optimization is needed of the processing of chitosan scaffolds.

Future Studies

Further research is needed to evaluate chitosan as a biomaterial used in scaffolding. Since ECs have been successfully seeded onto chitosan matrices before (31), ECs should be tried on the chitosan scaffolds to determine the cause of death of the cells. If the processing of the scaffolds is incorrect then this reseeding would result in dead ECs. Supplementing scaffolds with collagen or gelatin should also be investigated to determine if their presence increases the cells ability to attach. Wang *et al*. investigated a mixture of chitosan and collagen in periodontal cartilage tissue engineering with promising results (34). In addition, to increase strength of the scaffolds, genipin should be investigated as a possible cross-linking agent(35). This would allow for a stronger framework for the cells to attach and proliferate.

CHAPTER IV

EVALUATION OF COLLAGEN AS A TISSUE ENGINEERED SCAFFFOLD MATERIAL

Introduction

Relative to traditional methods of tissue engineering heart valves, a less traveled avenue is the method in which cells are entrapped in a gel. This form of tissue engineering relies on the established knowledge that cells embedded in collagen gels contract and compact the gels. The resulting compaction and contraction in turn increases the density of the collagen many folds (36). The process first involves mixing soluble, fibrillar collagen with the desired cell type. Once the collagen-cell mixture is neutralized, soluble collagen reassembles into fibrils and thus a gel is made. The desired cells within the gels begin to interact with the collagen fibrils and contract the gel. *In vitro* contraction shows similarities to wound healing *in vivo* (37). This method of tissue engineering is currently being applied in fabrication of blood vessels, mitral valve chordae and the development of heart valve leaflets in early stages.

Tissues of the body are in complex environments that can subject a tissue to various mechanical and biochemical factors that regulate the function of cells. The endocrine, autocrine and paracrine pathways along with ECM contacts send signals to cells under normal and pathological conditions. Thus to engineer a tissue ready for

implantation, the specimen must be pre-conditioned. This is done *in vitro* by subjecting the sample to biochemical factors and mechanical stimuli that are present *in vivo*.

Transforming growth factor- β_1 (TGF-β_1)

TGF-β_1 is a profibrotic cytokine that stimulates the production of ECM proteins in a number of different organ systems. This growth factor is secreted by a variety of cell types including vascular endothelial and smooth muscle cells with practically all cells having TGF-β_1 receptors. Since TGF-β_1 is secreted in an active form, it must be cleaved via the action of proteolytic enzymes, cell-cell interaction and acidification (38). It has also been seen to contribute to the increase of cell hypertrophy, polyploidy, and hypertension (39). Cipollone *et al.* reported that TGF-β_1 may be important in the stabilization of atherosclerotic plaques through the inhibition of local inflammation (40). However, an over expression of TGF-β_1 can lead to an excess amount of ECM protein production characteristic of fibrosis. In a tissue engineering setting, TGF-β_1 is known to vary cell proliferation and compaction of collagen gel constructs (41;42).

Platelet derived growth factor (PDGF)

The role of PDGF in soft tissues and bones has not been well established, but is known to be the first growth factor to initiate most wound healing. The growth factor attaches to transmembrane receptors on target cells when activated. PDGF is secreted by ECs, smooth muscle cells, and activated macrophages. It promotes smooth muscle cell migration, proliferation and matrix production associated with intimal thickening in arteriosclerosis. . The main function of PDGF is stimulating cellular replication. For this

reason, Stegemann *et al.* studied the effect of PDGF on collagen gels used in tissue engineering (41;42).

Matrix Metalloproteases

The purpose of pre-conditioning an engineered specimen is to initiate remodeling of ECM and degradation of the scaffold. Matrix Metalloproteases are proteolytic enzymes able to degrade various ECM proteins such as collagen, laminin, and fibronectin. Some MMPs are known to be collagenases, which cleave proteins at a small number of sites. This allows structural integrity of the matrix to be retained, while enabling cell migration. Other MMPs are less specific and are able to act where needed. This type of less specific MMP is vital to allow cells to divide when embedded in matrix. The activity of MMPs are rigorously controlled by mechanisms including local activation, confinement by cell-surface receptors, and secretion of inhibitors.

Hypothesis and Objective

I hypothesize that regular media in cyclic pressure will show the least amount of compaction with the highest ultimate tensile strength, TGF-β_1 will effect compaction and expression of MMPs, and PDGF will show minimal effects on remodeling potential. The objective of this study was to determine the optimal conditions required by collagen gels to produce a tissue engineered aortic heart valve. The affect of supplementing growth medium with TGF-β_1 or PDGF-BB and the addition of cyclic pressure was evaluated, with regard to remodeling potential.

Methods and Materials

Hydrogels were made using porcine aortic VICs. A suspension of 10^6 cells was made in 3X DMEM, 10% FBS, 2 mg/mL concentration of Type I collagen (BD Sciences, Franklin Lakes, NJ), and the appropriate amount of 0.1M NaOH to neutralize the solution (pH 7.0). Using a 12-well plate, approximately 1.25 mL of the solution was placed in each well and incubated at 37ºC for 1 hour. After one hour or once the gels had begun to solidify into a gelatinous state, the gels were immersed in 3 mL of complete media. The gels were allowed to sit undisturbed for 24 hours and were then liberated from the wells using a sterile scalpel. Gels were allowed to compact for 7 days, and were exposed to complete growth media, TGF-β_1 (human, Sigma, St. Louis, MO) supplemented and PDGF-BB (rat, Sigma, St. Louis, MO) supplemented complete media. The desired concentration of TGF-β_1 and PDGF-BB supplemented media was 2 and 5 ng/mL, respectively. These growth factors were reconstituted in 4mM HCl with 0.1% bovine serum albumin.

Test Conditions

Two different growth conditions were used to test the effects of cyclic pressure on the collagen gels. Static conditions were tested with the 12 well plates placed in an incubator at 37ºC and 5% CO_2 and the appropriate media being changed every 48 hours. A pressurized condition was also tested utilizing a pressure chamber within an incubator. The pressure chamber as seen in Figure 19 was made from acrylic. Two solenoid valves were used as exhaust and input. The input valve was connected to compressed air via a pressure regulator, and the exhaust was expelled into the incubator. The solenoid valves

were controlled via a LABView program in which the input valve would be activated for 0.6 seconds and the exhaust for 0.4 seconds. The input time was designed to mimic the aortic valve being closed during diastole, thereby increasing the pressure within the chamber. The exhaust time was based upon the drop of pressure experienced by the aortic valve when it is opened during systole. The valves were programmed to cycle at 1 Hz, which correlates to a heart rate of 60 beats per minute. A pressure transducer was used to convert pressure to a digital signal that was monitored by a LabVIEW program. The pressure range in which the gels were tested was 60-80 mmHg. Samples were placed in the pressure chamber for 7 days with the appropriate media being changed every 48 hours.

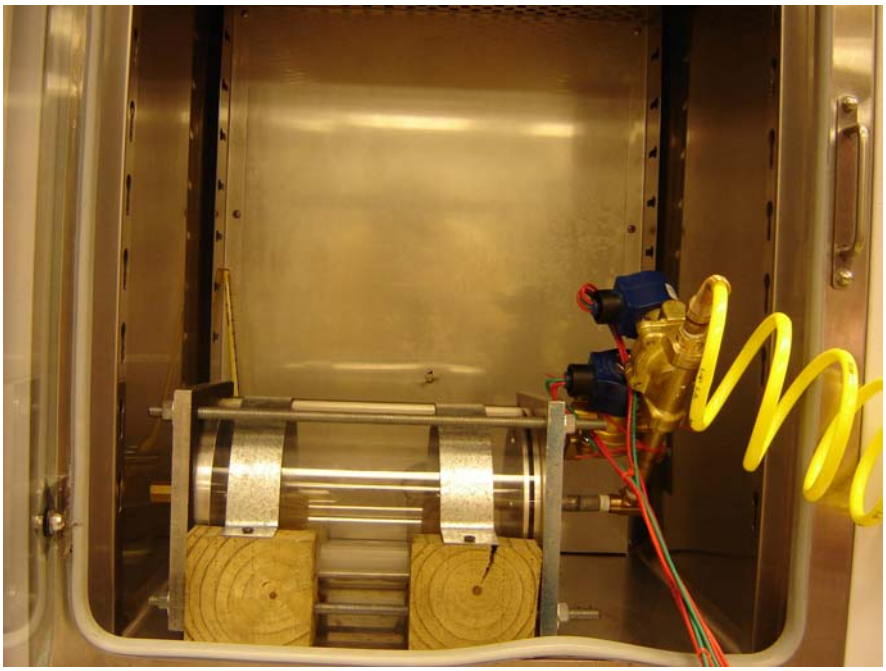

Figure 19 Pressure chamber used to expose gels to cyclic pressure over a 7 day period.

Compaction

Compaction was measured every two days using digital calipers and digital images. Using digital calipers, the disc were allowed to remain in complete media and measured being careful not to come in contact with the gel or media. In addition, digital images of the gels were taken with a ruler placed beside the 12 well plate. These images were imported into ImageJ (NIH) where a global scale was set by placing a line of a known pixel amount over the known length of the ruler. ImageJ was able to calculate the length of lines drawn over the diameter of the discs. Both methods of measurement were used every 2 days.

Gel Tensile Testing

After 7 days, the samples were removed from their respective conditions and a tensile strength test performed. Samples were cut into uniform 3.5mm strips and alligator clips were made to integrate into the MACH1 micromechanical testing system. For testing of the gels, a 1kg load cell was used. To test the samples, the load cell was first calibrated and then alligator clips were mounted. The samples were placed into the alligator clips as seen in Figure 20, care was taken to ensure an adequate amount of sample was clamped. The length between clamps was measured with digital calipers and recorded. The load cell and actuator position was zeroed. Cyclic tensioning at 1Hz was then performed to precondition the samples. A simple displacement of 100μm/s was conducted to pull the gels to failure. Load and position was recorded every tenth of a second and saved into a text file. Data analysis determined ultimate tensile strength and elastic moduli using Microsoft Excel.

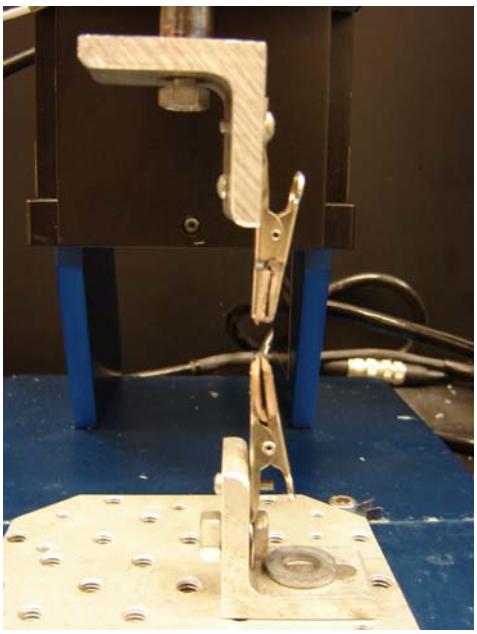

Figure 20 Alligator clips used to clamp collagen gels into MACH1 system to determine ultimate tensile strength

RNA isolation

RNA isolation was performed using an RNeasy kit from (Qiagen, Valencia, CA) according to the manufacturer's instructions. Briefly, gels were place into a 3mL tube and 300 µl of RLT Buffer was added. The gels were immediately homogenized until uniform. Next, 590 µl of double-distilled water and 10 µl of Proteinase K (20mg/mL in water, Promega, Madison, WI) were added to the homogenate. The tubes were then placed in a water bath at 55ºC for 10 minutes to activate Proteinase K. The supernatant was pipetted off and place into a microcentrifuge tube. To the supernatant, 0.5 volumes of 100% ethanol was added and mixed by pipetting. 700 µl of the samples were transferred into RNeasy mini columns in 2 mL collection tubes and centrifuged for 15

seconds at 10,000g. The liquid that passed through the columns was discarded. The columns were then filled with 700 µl of RW1 and centrifuged at 10,000g for 15 seconds. After centrifugation, the collection tubes were replaced and 500 µl of RPE was added to each column. The columns were then centrifuged for 15 seconds and the flow through was discarded. Another 500 µl of RPE was added to each column and centrifuged for 2 minutes. The flow through was discarded and the empty column was then centrifuged for 1 minute. The columns were then removed and placed into microcentrifuge tubes. Next, 50 µl of RNase-free water was added to each column and centrifuged for 1 minute. The RNeasy spin columns were then discarded and the tubes containing RNA were stored at -80ºC. The quality of isolated RNA isolated was assessed using a NanoDrop 1000 UV/Vis Spectrophometer. 1.5µl of isolated RNA was loaded onto the reading stage and samples were read. Levels were read at 260/280 with quality RNA deemed to have a ratio between 1.8-2.0. Also levels were also checked at 230 to assess the purity of RNA with values approximately 1.8 being pure RNA.

Quantitative Real Time Polymerase Chain Reaction

Quantitative RT-PCR was performed to measure the relative change in mRNA expression of genes MMP-1 and MMP-3, as previously reported(43). RT-PCR was carried out using the iScript One-Step RT-PCR kit with SYBR Green (Bio-Rad, Hercules, CA). A master mix was created using 0.25 µl SYBR Green One-Step Enzyme Mix, 6.25 µl 2X SYBR Green Reaction Mix, 0.25 µl of forward and reverse primers, seen in Table 3, and RNase/DNase-free distilled water to give a final volume of 11.5 µl per sample. The master mix was pippetted into a 96-well plate, and 1 µl of total RNA for

each sample was added, yielding a final reaction volume of 12.5 µl. cDNA synthesis and PCR amplification was performed using the following steps: 50ºC for 30 min; the reaction mixture was then heated to 95ºC for 5 min; a 60 cycle two-step PCR was then performed consisting of 95ºC for 15 seconds followed by 1 min at the annealing temperature, 55ºC. Reactions were carried out utilizing an i-Cycler Thermal Cycler (Bio-Rad, Hercules, CA).

Table 3 Primers for qRT-PCR to determine relative expression of MMP-1 and MMP-3

Gene Symbol	Primer Sequence 5'-3'
MMP-3 Left	TGTGGAGTTCCTGATGTTGG
MMP-3 Right	GGCTGAAGTCTCCGTGTTCT
MMP-1 Left	TTTCCTGGGATTGGCAAC
MMP-1 Right	TCCTGCAGTTGAACCAGCTA
18S Antisense	CGGGTCGGGAGTGGGTAAT
18S Sense	CGGAGAGGGAGCCTGAGAAA

Statistical and Data Analysis

Results of compaction data was processed in Microsoft Excel. Conclusions regarding gel compaction were made based off of paired t-test with a p-value <0.01 significant (n=12). Mechanical testing data was calculated using Microsoft Excel. Changes in UTS and elastic moduli were assessed for significance through paired t-test with p-values <0.1 considered significant (n=3). Also relative gene expression was calculated using Microsoft Excel. Experiments were run for each condition, and RNA was pooled from four samples. Relative expression was calculated assuming a 100% PCR efficiency using $2^{(\Delta C_T)}$ where C_T is the cycle threshold for the gene, and ΔC_T is the

difference between the house keeping gene, 18s, and the experimental groups. Means and paired t-test were calculated with significance determined based on a $p < 0.05$.

Results

Compaction of the scaffolds was recorded every other day over a 7 day period. The average diameter of the collagen gels is seen in Table 4. Statistical analysis was performed in Microsoft Excel and can be found in Figures 21, 22, and 23. Significant compaction was found throughout all treatment groups for the time period between Day 0 and Day 2 (p-value < 0.01). Gels subject to pressure in PDGF supplemented media showed the only significant compaction from Day 2 to Day 4. There was also significant compaction of all gels subjected to pressure from Day 4 to Day 6. However, only the PDGF supplemented samples in static conditions had a significant change in compaction over the same time period.

Table 4 Relative percent compaction over 7 days to determine the compaction of gels.

	Day 2	Day 4	Day 6
Regular static	50.9±0.02	47.8±0.04	50±0.03
Regular pressure	68.6±0.06	66.5±0.04	57.4±0.03
TGF static	36.9±0.03	38±0.04	34.8±0.02
TGF pressure	71.1±0.07	69.9±0.07	64.2±.09
PDGF static	39.6±0.03	39.2±0.02	42.9±0.02
PDGF pressure	65.1±0.03	57.8±0.03	52.6±0.02

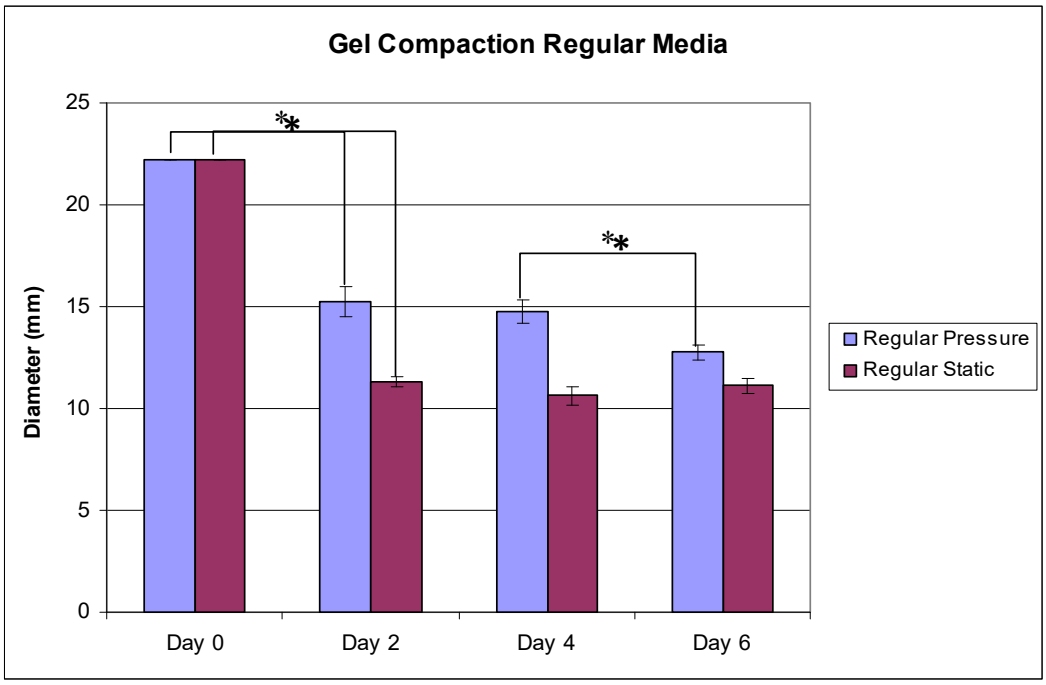

Figure 21 Gel compaction of collagen gels over 7 days in regular media and subjected to either static or cyclic pressure.

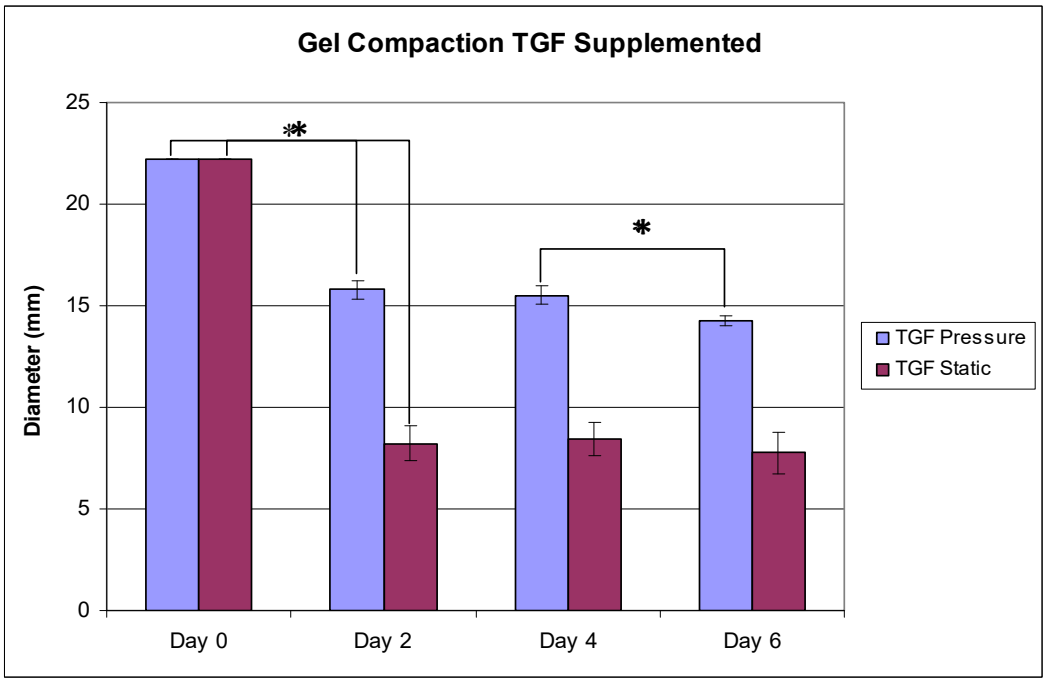

Figure 22 Gel compaction of gels in TGF supplemented media subjected to either static or cyclic pressure over 7 days.

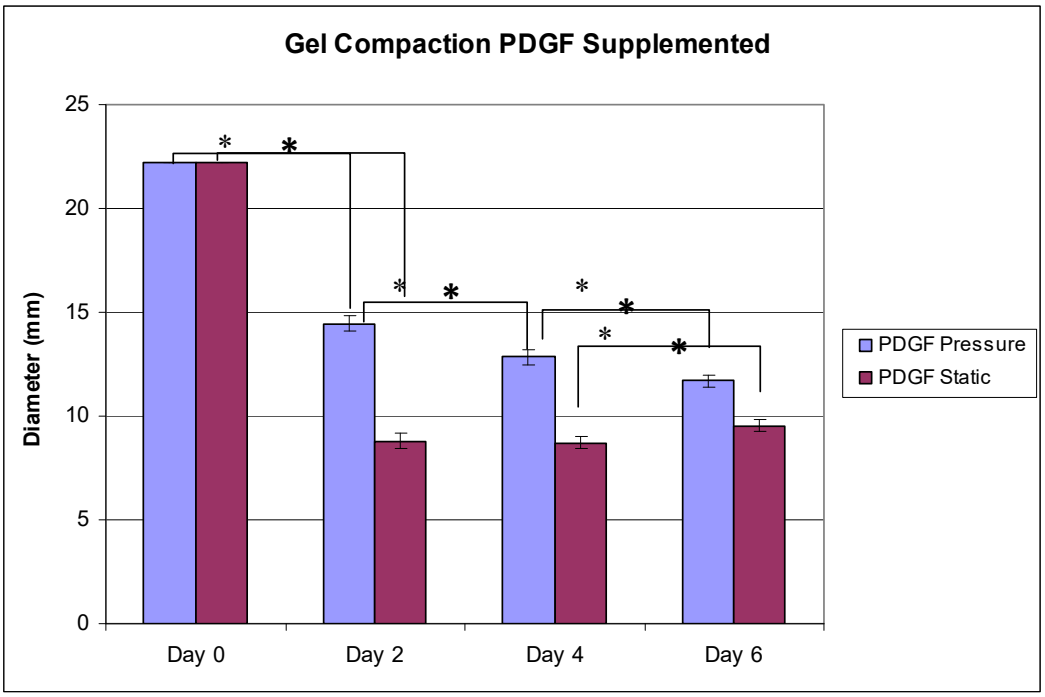

Figure 23 Compaction of collagen gels in PDGF supplemented media subjected to either static or cyclic pressure over 7 days.

The ultimate tensile strength and elastic modulus was measured for each treatment after 7 days. There was a statistically significant decrease in ultimate tensile strength in all treatments. In addition, only PDGF saw a significant decrease in the elastic modulus. The ultimate tensile strength comparison is shown in Figures 24, 25 and 26. Elastic moduli are compared between treatments in Figures 27, 28 and 29.

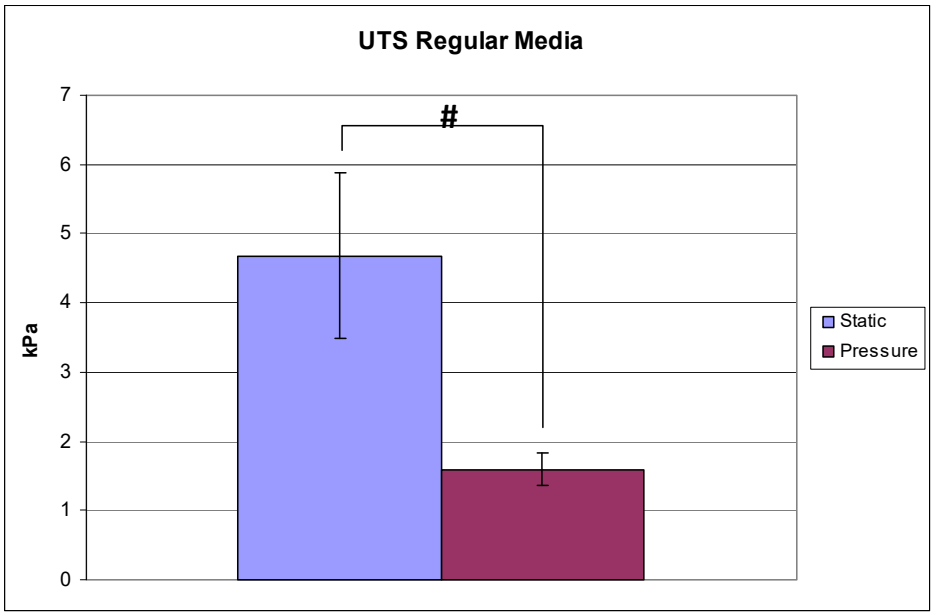

Figure 24 Graph comparing the ultimate tensile strength of collagen gels in regular media.

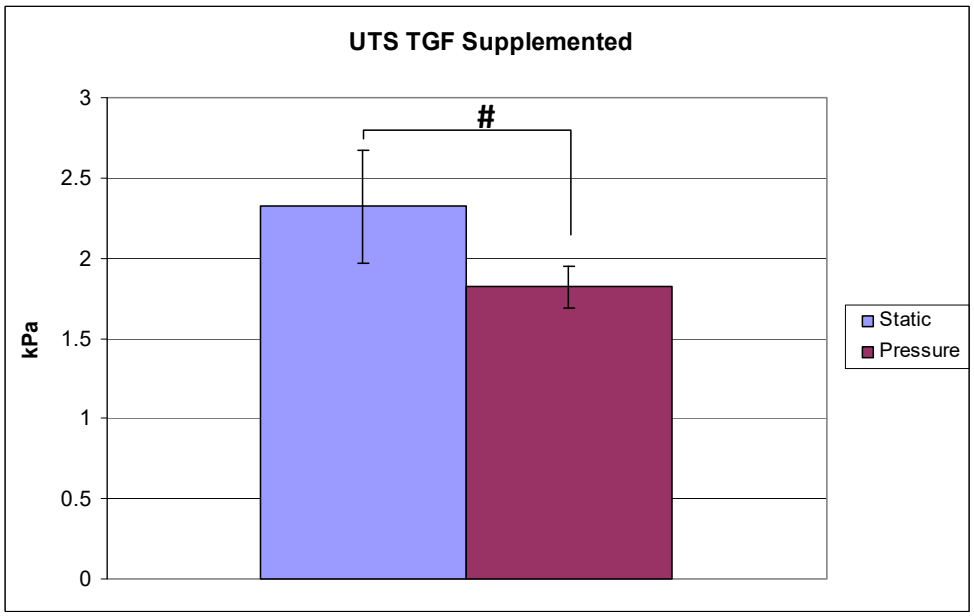

Figure 25 Graph comparing the ultimate tensile strength of collagen gels in TGF supplemented media.

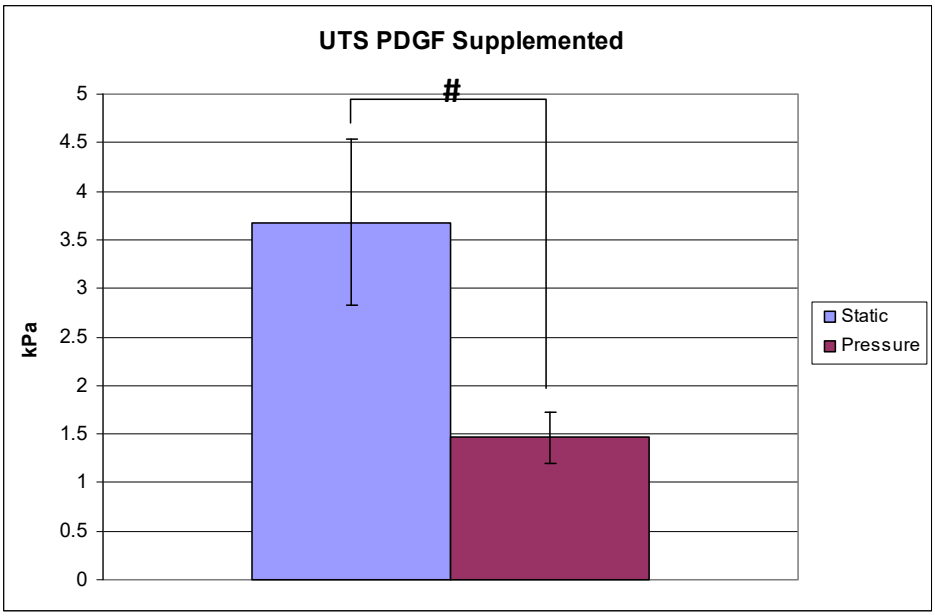

Figure 26 Graph comparing ultimate tensile strength of collagen gels in PDGF supplemented media.

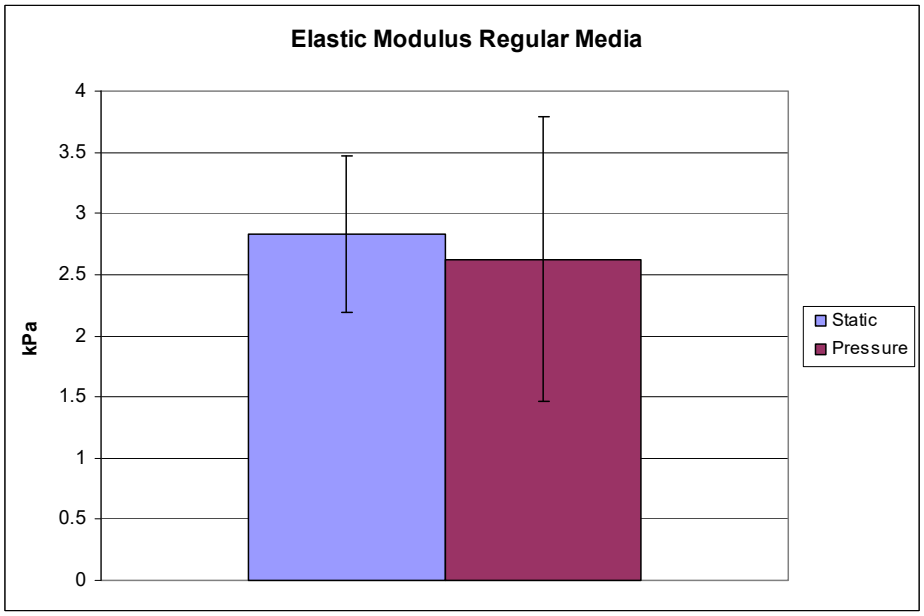

Figure 27 Graph comparing the elastic modulus of collagen gels in regular media.

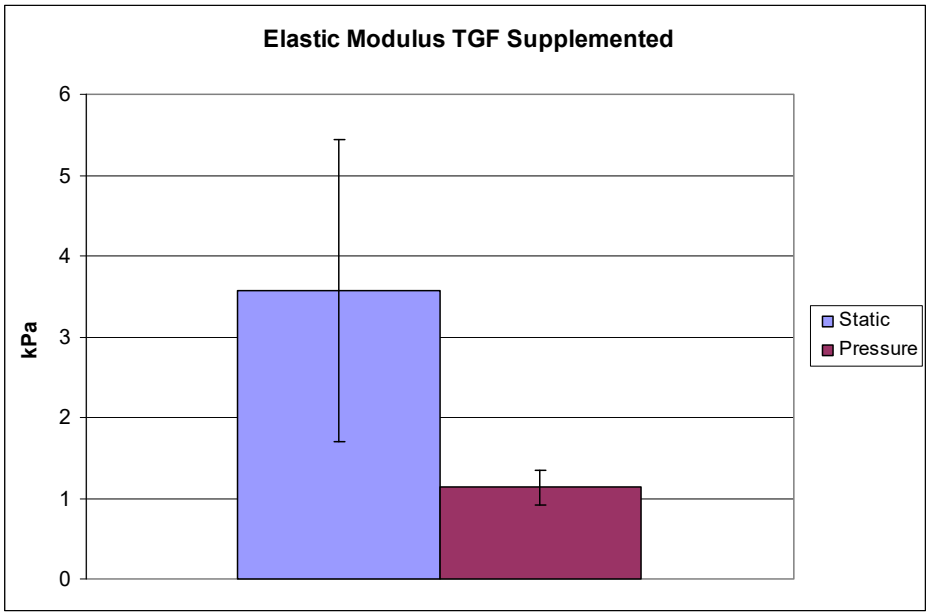

Figure 28 Graph comparing the elastic modulus of collagen gels in TGF supplemented media.

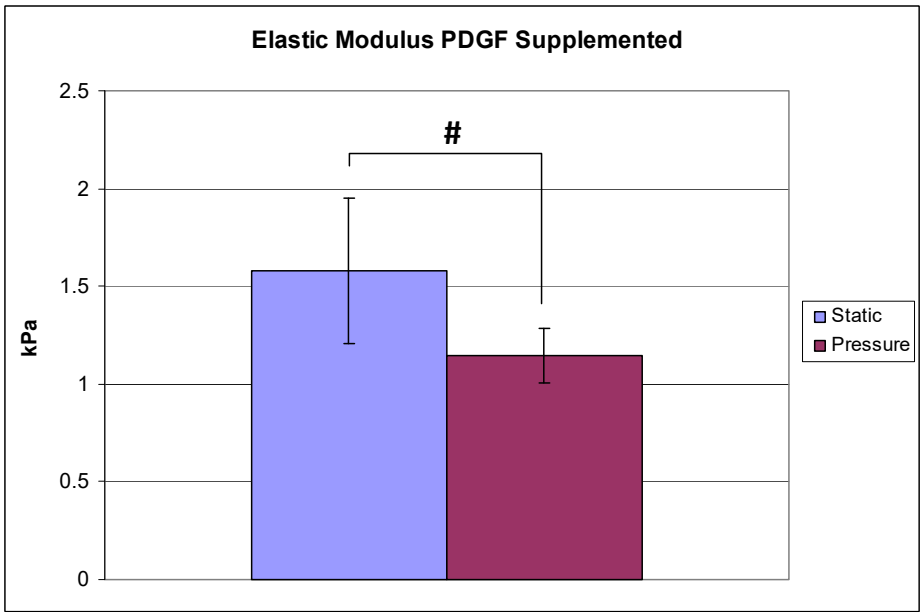

Figure 29 Graph comparing the elastic modulus of collagen gels in PDGF supplemented media.

Gene expression of MMP-1 and MMP-3 was measured using quantitative real time PCR. qRT-PCR data showed no measureable relative expression of MMP-1 or MMP-3 under static conditions over all treatments. MMP-1 and MMP-3 expression was evident in both regular and PDGF supplemented media, yet they showed no significant difference in expression. However, a 27.17 fold increase in MMP-1 and a 924 fold increase in MMP-3 relative gene expression was observed in samples supplemented with TGF under cyclic pressure. Gene expression data is shown in Figures 30 and 31.

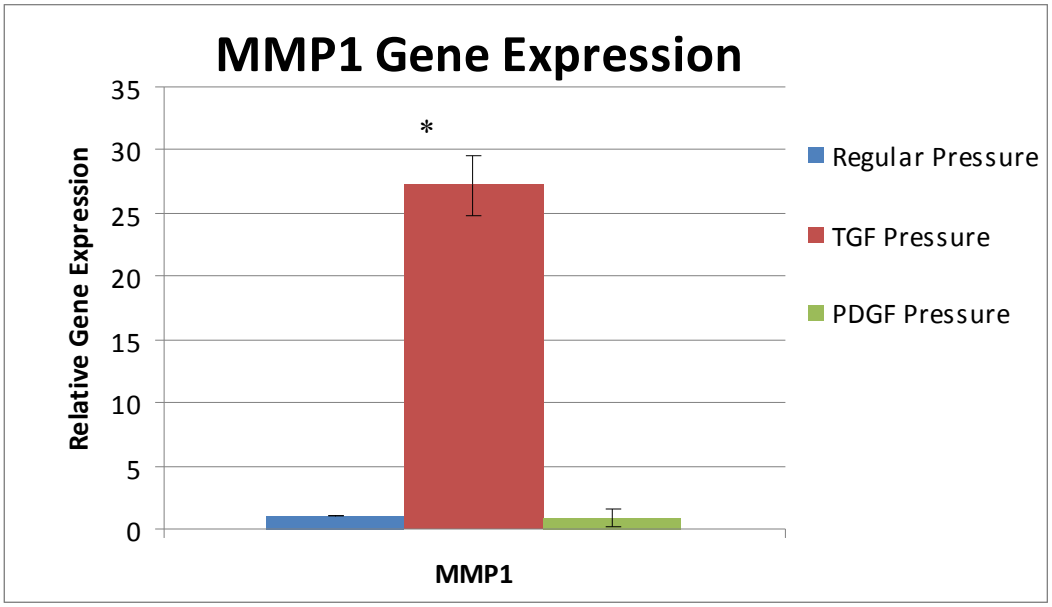

Figure 30 Graph of relative gene expression to determine the expression of MMP-1 in gels subjected to cyclic pressure.

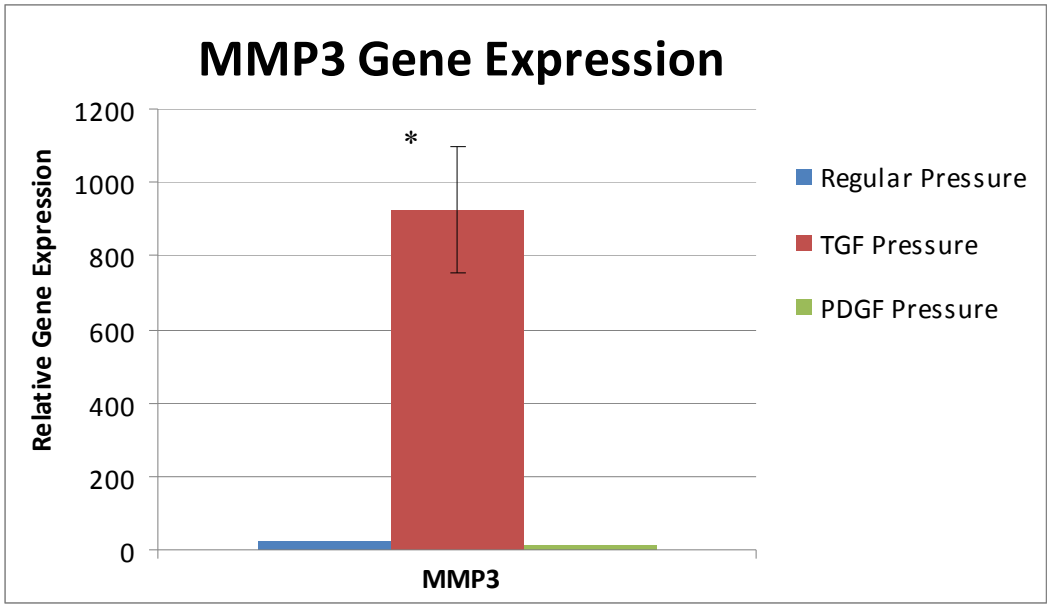

Figure 31 Graph of relative gene expression of MMP-3 in collagen gels exposed to cyclic pressure

Discussion

A thorough analysis of collagen gels as a potential scaffold for a tissue engineered heart valve was performed via seeding with valvular interstitial cells. Significant gel compaction was found from Day 0 to Day 2 throughout all treatment groups. This suggests there was instantaneous compaction activity of VICs regardless of pressure environment or media type. A differential time response was evident between groups at later time points. Gels subject to pressure in PDGF supplemented media showed the only significant compaction from Day 2 to Day 4. There was also significant compaction of all gels subjected to pressure from Day 4 to Day 6. This implies that application of cyclic pressure sustains VIC collagen compacting activity. PDGF appears to show more regulatory implications on compaction than TGF or normal growth media. This is further

evident due to the PDGF supplemented samples in static conditions from Day 4 to 6 had the only significant increase in gel diameter, thus decreasing compaction.

Digital imaging was the preferred method for obtaining compaction data. This method eliminated possible contamination by contacting the scaffold or media with the calipers. Also, images allowed for more precise measurement of the gel diameter. When using calipers, difficulty arose when gels would be in an awkward position and calipers could not align with the major axis of the collagen gels. Imaging allowed for a near instant diameter reading, minimizing the length of time the gels would be outside an incubator.

Mechanical properties were characterized to investigate the effects of the sample treatments on the structural integrity of the gels. A significant decrease in ultimate tensile strength was observed in all treatments subjected to cyclic pressure. In addition, only PDGF samples under pressure saw a significant decrease in the elastic modulus. This was possibly an artifact of a small sample size and large deviation.

Difficulties arose in the tensile testing of the gels. The diameter of the gels after 7 days is approximately 10 mm, rendering sample handling awkward and difficult. In addition, the clamps used for testing of chitosan scaffolds could not be employed due to the damage the clamps were causing to the gels and the size of collagen gel samples. Sample sizes were small, which necessitated the use of alligator clips, so clamping the appropriate amount of sample was tedious. Due to the elasticity of samples, tensioning to failure was problem. Often the samples would neck down but would not completely fail. The lack of a specific failure threshold and slippage resulted in disproportionate variance.

Real Time PCR was run to determine the amount of relative expression of MMP-1 and MMP-3. When a heart valve is actively remodeling, both MMPs are expressed. MMP-1 was investigated to determine the direct impact on collagen in the gels. The results of RT-PCR revealed that neither MMP-1 nor MMP-3 was expressed in static culture. This indicates that the constructs are not actively remodeling in static culture. However, the gels under pressure do not expel as much water content or contract as much as static gels, possibly to dampen the load experienced by gels under pressure. Under pressure, gels are actively remodeling, which is seen by the expression of both MMP-1 and MMP-3. A possible reason for the decrease in UTS is MMP-1, which is an interstitial collagenase that breaks down type I, II and III collagens, is expressed in samples subjected to cyclic pressure. MMP-3 was looked at to see general remodeling activity not directly influenced by type I rat tail collagen initially in the gels. MMP-3 was seen to be expressed even more than MMP-1, revealing that gels were actively remodeling the ECM. This activity, in addition to the effects of MMP-1, reduces the strength of gels when exposed to cyclic pressure.

Stegemann *et al.* investigated the effects of PDGF on vascular smooth muscle cells in collagen gels(42). They reported that when gels were mechanically stimulated by stretching and supplemented with PDGF, compaction was reduced. Interestingly, when VICs are exposed to similar conditions, as in the current study, compaction of collagen gels was reduced when exposed to PDGF and pressure. Stegemann postulated that reduced compaction was a result of MMPs being over-expressed, which is confirmed by the results of this study.

The lack of compaction raises an interesting question as to the impact on the gel as a whole. Since there is less compaction under pressure, this allows for more space in the matrix for cells to infiltrate and proliferate. By increasing proliferation, the amount of ECM produced by the cells will increase and will eventually lead to a stronger gel. Ultimately, a stronger gel would be closer to mimicking the native aortic valve leaflet. Overall, collagen gels are an exciting underdeveloped alternative material for use in tissue engineering.

Conclusion

Gels were pre-conditioned using biochemical factors and mechanical stimuli. Under static conditions gels all compacted significantly over the first 2 days that indicates a mechanism that causes gels to contract to an initial threshold. Over both test conditions the compaction of cells seemed to stabilize after the first 48 hours. Static gels in regular media showed the highest ultimate tensile strength; however, under pressure the strength of these gels was greatly reduced. Also gels in TGF-β_1 did demonstrate the most expression of MMPs under pressurized conditions. TGF-β_1 did contract the most under static conditions, but under pressure PDGF was the smallest disc. PDGF showed little expression of MMPs under pressure and no expression under static. Contrary to the hypothesis, PDGF showed significant change in compaction throughout the 7 day study. The gels under pressure showed less compaction, which meant that active remodeling was occurring. The lack of compaction is beneficial because the open space in the matrix allows more room for cells to infiltrate. As a result of more space, cells will have more space to proliferate, which in turn will eventually increase the overall strength of the gel

by the increased production of ECM. Overall, collagen gels show great potential as a scaffolding material for a tissue engineered heart valve.

Future Studies

A future study of a longer duration of the current experiment should be researched to determine if the collagen gel strength and compaction can recuperate after an extended exposure to cyclic pressure. Further research into the effects of various applied loads should be investigated. For example, gels should be subjected to three-dimensional loading via a vacuum pump system, FlexCell Tissue Train. Also, different types of collagen (I, II ,III, IV) should be evaluated as to determine the best option for making gels. Each type of collagen has unique properties that may have potential benefits in manufacturing a tissue engineered heart valve. In addition, mixtures of types of collagen should be included in the previously mentioned study. Further research should be conducted to determine if a better cell line exists for making collagen gels.

CHAPTER V

CONCLUSION

Tissue engineering is an emerging field that will have major impacts on the treatment of numerous ailments. One of the first steps of tissue engineering an implantable tissue is the design and fabrication of a scaffolding material. In this study, chitosan and collagen were investigated for their potential as scaffolding material.

Chitosan was found to be a material with many advantageous qualities including biocompatibility and biodegradation. The ease of processing and the abundant supply of chitosan make this material an enticing option for tissue engineering. However, for an application in the engineering of a heart valve chitosan still needs further investigation. The need to increase strength of the scaffold and increase the amount of viable cells are current limitations. With further exploration chitosan could possibly be an invaluable material in tissue engineering.

Collagen gels were pre-conditioned and assessed. Under pressure or mechanical stimuli gels expressed MMPs, which indicate remodeling activity. Also, media supplemented with growth factors effected the compaction of collagen gels. Samples exposed to cyclic pressure did not compact as rapidly as gels under static conditions. The lack of compaction leads to a more spacious matrix, which allowed for an increase in cell infiltration and proliferation. Collagen gels as scaffolding material showed great potential and should be further examined.

Overall, chitosan and collagen are exciting materials for use as scaffolds in a tissue engineered heart valve. Both have properties that make for an ideal substrate for numerous tissue engineering applications. With more exploration and optimization these materials could make the goal of engineering a heart valve a reality.

BIBLIOGRAPHY

(1) Yacoub MH, Cohn LH. Novel approaches to cardiac valve repair: from structure to function: Part I. Circulation 2004 Mar 2;109(8):942-50.

(2) Sacks MS, Smith DB, Hiester ED. The aortic valve microstructure: effects of transvalvular pressure
1. J Biomed Mater Res 1998 Jul;41(1):131-41.

(3) Vesely I. The role of elastin in aortic valve mechanics. J Biomech 1998 Feb;31(2):115-23.

(4) Deck JD. Endothelial cell orientation on aortic valve leaflets
1. Cardiovasc Res 1986 Oct;20(10):760-7.

(5) Butcher JT, Simmons CA, Warnock JN. Mechanobiology of the aortic heart valve. J Heart Valve Dis 2008 Jan;17(1):62-73.

(6) Simmons CA, Grant GR, Manduchi E, Davies PF. Spatial heterogeneity of endothelial phenotypes correlates with side-specific vulnerability to calcification in normal porcine aortic valves. Circ Res 2005 Apr 15;96(7):792-9.

(7) Schmitt-Graff A, Desmouliere A, Gabbiani G. Heterogeneity of myofibroblast phenotypic features: an example of fibroblastic cell plasticity. Virchows Arch 1994;425(1):3-24.

(8) Rabkin E, Hoerstrup SP, Aikawa M, Mayer JE, Jr., Schoen FJ. Evolution of cell phenotype and extracellular matrix in tissue-engineered heart valves during in-vitro maturation and in-vivo remodeling
1. J Heart Valve Dis 2002 May;11(3):308-14.

(9) Messier RH, Jr., Bass BL, Aly HM, Jones JL, Domkowski PW, Wallace RB, et al. Dual structural and functional phenotypes of the porcine aortic valve interstitial population: characteristics of the leaflet myofibroblast
3. J Surg Res 1994 Jul;57(1):1-21.

(10) Messier RH, Jr., Bass BL, Domkowski PW, Hopkins RA. Interstitial cellular and matrix restoration of cardiac valves after cryopreservation
1. J Thorac Cardiovasc Surg 1999 Jul;118(1):36-49.

(11) Bairati A, DeBiasi S. Presence of a smooth muscle system in aortic valve leaflets 1. Anat Embryol (Berl) 1981;161(3):329-40.

(12) Roy A, Brand NJ, Yacoub MH. Expression of 5-hydroxytryptamine receptor subtype messenger RNA in interstitial cells from human heart valves 11. J Heart Valve Dis 2000 Mar;9(2):256-60.

(13) Nishimura RA, McGoon MD, Schaff HV, Giuliani ER. Chronic aortic regurgitation: indications for operation--1988. Mayo Clin Proc 1988 Mar;63(3):270-80.

(14) Otto CM, Lind BK, Kitzman DW, Gersh BJ, Siscovick DS. Association of aortic-valve sclerosis with cardiovascular mortality and morbidity in the elderly 1. N Engl J Med 1999 Jul 15;341(3):142-7.

(15) Williams A, Davies S, Stuart AG, Wilson DG, Fraser AG. Medical treatment of Marfan syndrome: a time for change 2. Heart 2008 Apr;94(4):414-21.

(16) Vesely I. Heart valve tissue engineering 10. Circ Res 2005 Oct 14;97(8):743-55.

(17) Fallon AM, Marzec UM, Hanson SR, Yoganathan AP. Thrombin formation in vitro in response to shear-induced activation of platelets 2. Thromb Res 2007;121(3):397-406.

(18) Simmons CA, Grant GR, Manduchi E, Davies PF. Spatial heterogeneity of endothelial phenotypes correlates with side-specific vulnerability to calcification in normal porcine aortic valves 1. Circ Res 2005 Apr 15;96(7):792-9.

(19) Rabkin E, Schoen FJ. Cardiovascular tissue engineering 3. Cardiovasc Pathol 2002 Nov;11(6):305-17.

(20) Hutmacher D, Hurzeler MB, Schliephake H. A review of material properties of biodegradable and bioresorbable polymers and devices for GTR and GBR applications 1. Int J Oral Maxillofac Implants 1996 Sep;11(5):667-78.

(21) Riddick DH, DeGrazia CT, Maenza RM. Comparison of polyglactic and polyglycolic acid sutures in reproductive tissue 1. Fertil Steril 1977 Nov;28(11):1220-5.

(22) Stock UA, Vacanti JP, Mayer Jr JE, Wahlers T. Tissue engineering of heart valves -- current aspects 8. Thorac Cardiovasc Surg 2002 Jun;50(3):184-93.

(23) Williams SF, Martin DP, Horowitz DM, Peoples OP. PHA applications: addressing the price performance issue: I. Tissue engineering
1. Int J Biol Macromol 1999 Jun;25(1-3):111-21.

(24) Tomihata K, Ikada Y. In vitro and in vivo degradation of films of chitin and its deacetylated derivatives. Biomaterials 1997 Apr;18(7):567-75.

(25) Pangburn SH, Trescony PV, Heller J. Lysozyme degradation of partially deacetylated chitin, its films and hydrogels. Biomaterials 1982 Apr;3(2):105-8.

(26) Boot RG, Renkema GH, Strijland A, van Zonneveld AJ, Aerts JM. Cloning of a cDNA encoding chitotriosidase, a human chitinase produced by macrophages
9. J Biol Chem 1995 Nov 3;270(44):26252-6.

(27) Jiankang H, Dichen L, Yaxiong L, Bo Y, Hanxiang Z, Qin L, et al. Preparation of chitosan-gelatin hybrid scaffolds with well-organized microstructures for hepatic tissue engineering
1. Acta Biomater 2008 Jul 17.

(28) Nettles DL, Elder SH, Gilbert JA. Potential use of chitosan as a cell scaffold material for cartilage tissue engineering
2. Tissue Eng 2002 Dec;8(6):1009-16.

(29) Oliveira SM, Mijares DQ, Turner G, Amaral IF, Barbosa MA, Teixeira CC. Engineering Endochondral Bone: In Vivo Studies
2. Tissue Eng Part A 2008 Aug 31.

(30) Blan NR, Birla RK. Design and fabrication of heart muscle using scaffold-based tissue engineering. J Biomed Mater Res A 2007 Oct 30.

(31) Cuy JL, Beckstead BL, Brown CD, Hoffman AS, Giachelli CM. Adhesive protein interactions with chitosan: consequences for valve endothelial cell growth on tissue-engineering materials
2. J Biomed Mater Res A 2003 Nov 1;67(2):538-47.

(32) Wan Y, Fang Y, Wu H, Cao X. Porous polylactide/chitosan scaffolds for tissue engineering
3. J Biomed Mater Res A 2007 Mar 15;80(4):776-89.

(33) Liao J, Joyce EM, Sacks MS. Effects of decellularization on the mechanical and structural properties of the porcine aortic valve leaflet
2. Biomaterials 2008 Mar;29(8):1065-74.

(34) Peng L, Cheng XR, Wang JW, Xu DX, Wang G. Preparation and evaluation of porous chitosan/collagen scaffolds for periodontal tissue engineering
1. Journal of Bioactive and Compatible Polymers 2006 May;21(3):207-20.

(35) Moura MJ, Figueiredo MM, Gil MH. Rheological study of genipin cross-linked chitosan hydrogels
1. Biomacromolecules 2007 Dec;8(12):3823-9.

(36) Tranquillo RT, Girton TS, Bromberek BA, Triebes TG, Mooradian DL. Magnetically orientated tissue-equivalent tubes: application to a circumferentially orientated media-equivalent
1. Biomaterials 1996 Feb;17(3):349-57.

(37) Guidry C, Grinnell F. Contraction of hydrated collagen gels by fibroblasts: evidence for two mechanisms by which collagen fibrils are stabilized
2. Coll Relat Res 1987 Feb;6(6):515-29.

(38) Petrov VV, van Pelt JF, Vermeesch JR, Van D, V, Vekemans K, Fagard RH, et al. TGF-beta1-induced cardiac myofibroblasts are nonproliferating functional cells carrying DNA damages
1. Exp Cell Res 2008 Apr 15;314(7):1480-94.

(39) Fukuda N. Molecular mechanisms of the exaggerated growth of vascular smooth muscle cells in hypertension. J Atheroscler Thromb 1997;4(2):65-72.

(40) Cipollone F, Fazia M, Mincione G, Iezzi A, Pini B, Cuccurullo C, et al. Increased expression of transforming growth factor-beta1 as a stabilizing factor in human atherosclerotic plaques. Stroke 2004 Oct;35(10):2253-7.

(41) Stegemann JP, Nerem RM. Altered response of vascular smooth muscle cells to exogenous biochemical stimulation in two- and three-dimensional culture. Exp Cell Res 2003 Feb 15;283(2):146-55.

(42) Stegemann JP, Nerem RM. Phenotype modulation in vascular tissue engineering using biochemical and mechanical stimulation. Ann Biomed Eng 2003 Apr;31(4):391-402.

(43) Warnock JN, Burgess SC, Shack A, Yoganathan AP. Differential immediate-early gene responses to elevated pressure in porcine aortic valve interstitial cells
7. J Heart Valve Dis 2006 Jan;15(1):34-41.